NPS-MAE-10-001

NAVAL POSTGRADUATE SCHOOL

MONTEREY, CALIFORNIA

Characterization of Carbon Nanotube-enhanced Water as a Phase Change Material for Thermal Energy Storage Systems

by

Brian Ryglowski, Young W. Kwon, and Randall D. Pollak

4 January 2010

Approved for public release; distribution is unlimited

Prepared for: Northrop Grumman Systems Corporation, Electric Systems Sector (NGES)
Marine Systems Business Unit, 4010 East Hendy Avenue, Sunnyvale, CA 94088 -3499

NAVAL POSTGRADUATE SCHOOL
Monterey, California 93943-5000

Daniel T. Oliver
President

Leonard A. Ferrari
Executive Vice President and
Provost

This report was prepared for Northrop Grumman Systems Corporation, Electric Systems Sector and funded by NCRADA-NPS-09-0136.

This report was prepared by:

_____
Brian K. Ryglowski
Lieutenant, United States Navy

_____
Young W. Kwon
Professor
Dept. of Mechanical and
Astronautical Engineering

_____
Randall D. Pollak
Major, United States Air Force
Dept. of Mechanical and
Astronautical Engineering

Reviewed by:

_____
Knox T. Millsaps
Chairman
Department of Mechanical and
Astronautical Engineering

Released by:

_____
Karl van Bibber
Vice President and Dean of Research

REPORT DOCUMENTATION PAGE

Form Approved
OMB No. 0704-0188

1. REPORT DATE	**2. REPORT TYPE**	**3. DATES COVERED** *(From - To)*
4 January 2010	Technical Report	April 2009 - Jan 2010

4. TITLE AND SUBTITLE
Characterization of Carbon-Nanotube-enhanced Water as a Phase Change Material for Thermal Energy Storage Systems

5a. CONTRACT NUMBER
NCRADA-NPS-09-0136

5b. GRANT NUMBER

5c. PROGRAM ELEMENT NUMBER

6. AUTHOR(S)
Brian Ryglowski, Young W. Kwon and Randall D. Pollak

5d. PROJECT NUMBER

5e. TASK NUMBER

5f. WORK UNIT NUMBER

7. PERFORMING ORGANIZATION NAME(S) AND ADDRESS(ES)
Naval Postgraduate School
Monterey, CA 93943

8. PERFORMING ORGANIZATION REPORT NUMBER
NPS-MAE-10-001

9. SPONSORING / MONITORING AGENCY NAME(S) AND ADDRESS(ES)
Northrop Grumman Systems Corporation, Electric Systems Sector, Sunnyvale, CA 97088

10. SPONSOR/MONITOR'S ACRONYM(S)

11. SPONSOR/MONITOR'S REPORT NUMBER(S)

12. DISTRIBUTION / AVAILABILITY STATEMENT
Approved for public release; distribution is unlimited

13. SUPPLEMENTARY NOTES The views expressed in this report are those of the author and do not reflect the official policy or position of the Department of Defense or the U.S. Government.

14. ABSTRACT Innovation in electronics and directed energy technologies is accelerating as the 21st century progresses. The requirement to process, store and interpolate information and signals faster and with compact electronic units has led to the engineering of high power electronics. As the power density of these electronic systems increases, the demand for cooling increases. Development of directed energy systems also requires the dissipation of large heat loads. If the heat generated by high power electronics and other high energy systems is not reduced or transferred efficiently and quickly, resultant pre-mature equipment failure, individual component failure or the inability to operate the equipment will occur.

Carbon nanotube enhanced fluids have shown increases in the thermal conductivity from 20% to 250% when compared to the base heat transfer fluid. This study focuses on the stability of static, water-based, carbon nanotube enhanced mixtures during thermal cycling (i.e., freezing and thawing) of the nanofluid using various types of carbon nanotubes, loading percentages and surfactants. Electrical resistance measurements were recorded over a series of phase changes in order to assess the stability of the nanofluid.

Experimental results showed that static, carbon nanotube enhanced nanofluids are stable between three to five freeze and thaw cycles before the carbon nanotubes start to agglomerate and subside. This resulted in an increased electric conductivity, and validated the use of electrical resistance measurements as a viable means of assessing the stability of the nanofluid. However, ultrasonication of the nanofluids after the instability recovers the original electric conductivity of the nanofluid.

15. SUBJECT TERMS Carbon Nanotube, Thermal Energy Storage Systems, Characterization of Nanofluids, Static Phase Change Materials, Heat Transfer Nanofluid Systems

16. SECURITY CLASSIFICATION OF:			**17. LIMITATION OF ABSTRACT**	**18. NUMBER OF PAGES**	**19a. NAME OF RESPONSIBLE PERSON**
a. REPORT Unclassified	**b. ABSTRACT** UU	**c. THIS PAGE** U	Unclassified		**19b. TELEPHONE NUMBER** *(include area code)*

Standard Form 298 (Rev. 8-98)
Prescribed by ANSI Std. Z39.18

THIS PAGE INTENTIONALLY LEFT BLANK

ABSTRACT

Innovation in electronics and directed energy technologies is accelerating as the 21st century progresses. The requirement to process, store and interpolate information and signals faster and with compact electronic units has led to the engineering of high power electronics. As the power density of these electronic systems increases, the demand for cooling increases. Development of directed energy systems also requires the dissipation of large heat loads. If the heat generated by high power electronics and other high energy systems is not reduced or transferred efficiently and quickly, resultant pre-mature equipment failure, individual component failure or the inability to operate the equipment will occur.

Carbon nanotube enhanced fluids have shown increases in the thermal conductivity from 20% to 250% when compared to the base heat transfer fluid. This study focuses on the stability of static, water-based, carbon nanotube enhanced mixtures during thermal cycling (i.e., freezing and thawing) of the nanofluid using various types of carbon nanotubes, loading percentages and surfactants. Electrical resistance measurements were recorded over a series of phase changes in order to assess the stability of the nanofluid.

Experimental results showed that static, carbon nanotube enhanced nanofluids are stable between three to five freeze and thaw cycles before the carbon nanotubes start to agglomerate and subside. This resulted in an increased electric conductivity, and validated the use of electrical resistance measurements as a viable means of assessing the stability of the nanofluid. However, ultrasonication of the nanofluids after the instability recovers the original electric conductivity of the nanofluid.

THIS PAGE INTENTIONALLY LEFT BLANK

TABLE OF CONTENTS

LIST OF ACRONYMS AND ABBREVIATIONS

AC	Alternating Current
ASTM	American Society of Testing and Materials
C	Clear
CNT	Carbon Nanotube
DC	Direct Current
H	Homogenous
HS	Heavy Sediment
LA	Large Agglomerates
LDS	Lithium Dodecyl Sulfate
LS	Light Sediment
MA	Medium Agglomerates
MWCNT	Multi-wall Carbon Nanotube
NPS	Naval Postgraduate School
S	Sediment
SA	Small Agglomerates
SEM	Scanning Electron Microscope
SWCNT	Single Wall Carbon Nanotube
VOL	Volume
VSA	Very Small Agglomerates

THIS PAGE INTENTIONALLY LEFT BLANK

I. INTRODUCTION

A. THERMAL MANAGEMENT PROBLEM FOR DENSE, HIGH POWER ELECTRONICS AND DIRECTED ENERGY SYSTEMS

Innovation in electronics and directed energy technologies is accelerating as the 21st century progresses. The requirement to process, store and interpolate information and signals faster and with compact electronic units has led to the engineering of high power electronics. As the power density of these electronic systems increases, the demand for cooling increases. Development of directed energy systems also requires the dissipation of large heat loads. If the heat generated by high power electronics and other energy systems is not reduced or transferred efficiently and quickly, resultant pre-mature equipment failure, individual component failure or the inability to operate the equipment will occur. This problem can be solved by using large, elaborate cooling system arrangements with modern technology but defeats the purpose of using a compact unit.

In order to reduce the size, weight and cooling system complexity an efficient and effective means of heat transfer must exist. Optimization of cooling mediums, flow rates, ancillary equipment requirements and installation space restrictions must be taken into account. Conventional methods to increase cooling rates include using extended fin surfaces or microchannels within the cooling assembly. Another approach has revolved around increasing the thermal conductivity of the cooling medium. By improving the thermal properties of the cooling medium, the effective size of the cooling system arrangement can be scaled down to meet various space restrictions.

The inherent properties of water, oil and ethylene glycol mixtures render them as relatively poor heat transfer fluids. Maxwell's theoretical work first alluded to using solid-liquid mixtures to improve the heat transfer properties of conventional fluids since the thermal conductivity of solids is significantly higher than that of liquids [1]. Since then, many studies on the effects of metallic-based nanoparticles suspended in heat transfer fluids have shown a significant improvement in the thermal conductivity of the

fluid [2]. This scientific achievement in the use and application of nanoparticles has laid the foundation for future experiments using nanoparticles and their effects in heat transfer in high power density systems.

B. APPLICATION OF NANOPARTICLES AND THEIR USE IN NANOFLUIDS

Nanofluids are a new class of solid-liquid mixtures consisting of solid particles with diameter sizes on the order of 1 to 100 nanometers (nm) suspended in a heat transfer medium. Some common metallic and non-metallic solids that have been used in nanofluid research include but are not limited to silver, copper, aluminum, diamond, silicon, alumina, and carbon nanotubes. Common heat transfer mediums include water, ethylene glycol and engine oil [3].

Nanofluid research is a growing field and has focused primarily on the improvements in heat transfer properties of the nanofluid. Advantages to using nanofluids include higher cooling rates, smaller and lighter cooling systems, a reduced inventory of heat transfer fluid and miniaturization of individual heat exchangers [3], [4], [5]. However, as studies progress, there are still difficulties in dealing with nanofluids such as ensuring a homogenous dispersion of the nanoparticles throughout the heat transfer fluid, controlling processing techniques for the nanoparticles and understanding the physics of nanoparticle behavior.

Initial studies conducted by Choi et al. [6] showed significant increases in the thermal conductivity of a nanofluid using copper nanoparticles. When comparing the thermal conductivity of metallic and non-metallic solids to various non-metallic heat transfer fluids, solids exhibited thermal conductivities orders of magnitude higher than the base fluid. By adding a more conductive material (metallic or non-metallic solid) to a lower conducting heat transfer fluid, studies could focus on the resultant thermal conductivity properties of the nanofluid.

The improvement in the thermal conductivity of nanofluids can be attributed to the interfacial resistance and the resistance within the nanoparticle microstructure. Each plays an important role in the resistance to heat flow. Regardless of the type and size of nanoparticle, any interface at the microstructure is a barrier for heat flow. As the interface distance between

the nanoparticle and heat transfer fluid decreases or the thickness (diameter) of a nanoparticle decreases, the resistance drop across the particle also decreases. The high surface-to-volume ratio of nanoparticles decreases the overall particle resistance and enables them to be effective conductors. On a nano-scale level, the resistance at the surface of a nanoparticle is almost equivalent to the resistance of the particle itself. Therefore, the overall heat transfer becomes comparable to the nanoparticle microstructure and the conduction paths formed by dispersed nanoparticles [7].

C. CARBON NANOTUBE ENHANCED FLUIDS

1. Carbon Nanotubes

Carbon nanotubes (CNT) were first discovered by S. Iijima in 1991 [8]. CNTs are a member of the fullerene family and are also an allotrope of carbon called graphene. Graphene is a densely packed single, hexagonal layer of carbon-bonded atoms that are rolled to form a cylindrical microstructure. The ends of the cylindrical microstructure can be capped with a hemispherical structure from the fullerene family or left open. The orientation of the graphene microstructure gives CNT's their unique strength, electrical and thermal properties. Figure 1 illustrates the microstructure of a single graphene layer rolled in different orientations [9].

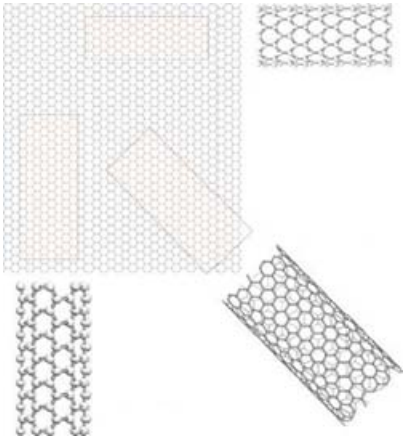

Figure 1. Graphene Sheet Rolled into Carbon Nanotubes.

The two main types of carbon nanotubes are single wall carbon nanotubes (SWCNT) and multi-wall carbon nanotubes (MWCNT). SWCNTs are composed of a

single sheet of graphene rolled into a cylinder capped with one-half of a fullerene molecule at each end of the cylinder. A MWCNT consists of concentric sheets of rolled graphene that are either capped with one-half a fullerene molecule at each end or left open. See Figure 2 for an illustration of a SWCNT and MWCNT [10]. For more information regarding CNT structure, physical properties and synthesis (growth), see reference [11].

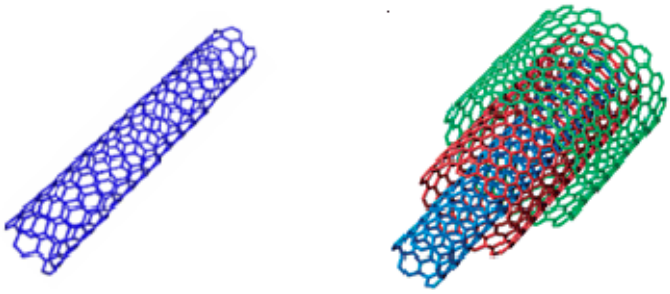

Figure 2. (Left) SWCNT. (Right) MWCNT.

Valence bond theory, or orbital mixing, explains why carbon nanotubes can form various microstructure orientations. Each carbon atom has six electrons which occupy the $1s^2$, $2s^2$ and $2p^2$ orbitals. The $1s^2$orbital contains two strongly bound electrons where as the $2s^2$ and $2p^2$ orbital contain four weakly bonded valence electrons. These four electrons can readily mix with each other or bond with neighboring carbon atoms (hybridization) to form various planar bonds, also known as sp^2 bonds [11].

The orientation of planar bonds between carbon atoms affects the overall energy state of the CNT, which directly impacts the thermal and electrical conductivity of the CNT. In general, a higher energy state carbon atom will have a higher conductivity than a lower energy state carbon atom. The detailed explanation of the electrical properties of various band structures is beyond the scope of this study, but is described in reference [11].

2. Carbon Nanotube-based Nanofluids

Numerous investigations on the improvement of the thermal conductivity of heat transfer fluids using solid particles have been conducted since Maxwell's theoretical observations in 1904 [1]. Using Choi's initial results with solid, metallic nanoparticles

[6], he and others studied the effects of using multiple types of CNTs from different synthesis processes using various dispersion techniques in multiple heat transfer fluids [6], [12], [13], [14], [15]. Those studies have shown increases in the thermal conductivity of the nanofluid ranging from 20% to 250% when compared to the base heat transfer fluid. Although theoretical calculations and modeling based upon experimental data have not been able to accurately predict the thermal conductivity of CNT enhanced nanofluids given various parameters, experimental results clearly demonstrate that CNT suspensions drastically improve the thermal properties of existing heat transfer fluids.

The intensive thermal and electrical properties of CNTs make them an appealing candidate for their use in nanofluids. However, the molecular attractive forces, or Van der Waals forces, between CNTs pose a significant problem in effectively employing CNTs in a heat transfer liquid. Since CNTs are unable to form strong bonds with their surroundings when placed in a liquid, they tend to form agglomerates, or large masses, with neighboring nanotubes. Various dispersion methods have been used to ensure a homogenous dispersion of the CNTs throughout the nanofluid.

CNT dispersion is accomplished by physical or chemical means. Physical dispersion techniques include high speed shearing of the nanofluid using mechanical mixing techniques, ball milling or grinding of CNTs prior to their addition into the nanofluid, and ultrasonication of the nanofluid. Chemical dispersion techniques include the chemical modification of the CNT surface during synthesis and use of surfactants to lower the interfacial tension of the heat transfer liquid and CNTs. The most stable suspensions have been achieved by using a combination of both physical and chemical techniques [16].

3. The Relationship between Thermal and Electrical Conductivity

The strong atomic bonds between carbon atoms enable it to have excellent conductive properties. The Wiedemann-Franz law is an empirical law of physics that states that the thermal and electrical conductivity properties are directly related by a constant multiplied by the absolute temperature of the metal. This is also known as the Lorentz relation [17, 18]. A linear relationship between the thermal conductivity and

material absolute temperature has been proven in many studies of various metallic and semi-conducting materials. However, electrical conductivity testing of the same materials fails to yield the same linear relationship. Despite inconsistent results from various electrical conductivity tests, the conductivity does, in fact, increase with an increasing absolute temperature [18]. By applying this relationship to nanofluids, the thermal conductivity improvements achieved from using CNTs can be directly associated to improvements in the electrical conductivity of the nanofluid.

4. Naval Postgraduate School Previous Research

In June of 2008, Kuhlmann studied the various thermal and fluid properties of CNT-enhanced nanofluids and their possible inclusion in advanced thermal management systems. He evaluated various CNT loading concentrations, temperature profiles, various ultrasonication settings and surfactant concentrations. The study also focused on the development of an appropriate protocol for producing stable, colloidal CNT suspensions. His thermal analysis of the nanofluids revealed that CNTs possess a sensitive architecture composed of loosely connected nanotube networks that directly impact the conductivity properties of the nanofluid [19].

D. PROJECT CONCEPT

The goal of this study is to evaluate the stability of static, CNT-enhanced, water-based nanofluids over a specified number of thermal cycles, or phase changes between freeze and thaw. The stability of the CNT-enhanced nanofluid is based upon changes in the conductive paths formed by the homogenous dispersion of the nanotube network. Theoretically, if the dispersed nanotubes maintained a homogenous network, the conductive properties of the nanofluid would remain intact. Any changes in the conductive properties during the thermal cycling of the nanofluid would indicate a change within the nanotube network.

The electrical conductivity of the nanofluid will be used to assess the stability of the nanofluid throughout thermal cycling. This study focuses on the ability to measure electrical resistance to accurately detect changes in the CNT network. This study will also

evaluate the effects of CNT concentration, type of CNT, type of surfactant and the nanofluid temperature during preparation on the electrical conductivity and stability of the nanofluid.

Secondary studies were also conducted using electrical resistance measurements to evaluate the stability of the surfactant during thermal cycling, and the effects of combining different types of CNTs in the nanofluid.

THIS PAGE INTENTIONALLY LEFT BLANK

II. EXPERIMENTAL APPROACH AND VALIDATION

A. DESIGN OF EXPERIMENT

Based on the results of previous research using CNT-enhanced nanofluids, the variables that had a significant impact on the thermal conductivity properties of a nanofluid are:

- Type of Base Fluid
- Type of CNT
- CNT Volumetric Loading Percentage (Concentration)
- Type of Surfactant
- Surfactant Volumetric Loading Percentage (Concentration)
- Size, or Aspect Ratio, of CNT

A factorial approach was used to develop an experimental matrix. Each parameter would have two levels, or settings. With the aim of keeping focus on the stability of the nanofluid, some parameters were fixed to reduce the number of samples that needed to be prepared. The base fluid, surfactant loading percentage and CNT size were fixed so as to only have one level. Utilizing the Kuhlmann findings in the NPS 2008 study, similar processing techniques and comparable CNT and surfactant loadings were selected in order to produce a stable nanofluid. Table 1 lists the design parameters for this study.

Table 1. Design Parameters for Thesis Research

Parameter	Level	Settings
CNT Type	2	SWCNT MWCNT
CNT Loading	2	0.1 % volume 0.2% volume
Surfactant Type	2	Lithium Dodecyl Sulfate (LDS) Igepal
Base Fluid	1	Distilled Water
Surfactant Loading	1	3.0% volume
CNT Size	1	SWCNT: 1—10μm x 1nm MWCNT: 5—20μm x 15 +/- 10nm

B. PROPERTIES OF SELECTED PARAMETERS

1. Heat Transfer Fluid

The heat transfer fluid used for this research was distilled water. The excellent thermal conductivity properties, specific heat and latent heat of fusion characteristics make it a favorable choice in many heat transfer systems including high power electronics and directed energy systems. Table 2 lists some important properties of distilled water [20].

Table 2. Properties of Distilled Water

Parameter	Value
Density	liquid: 1000 kg/m^3 solid: 917 kg/m^3
Melting Point	0 °C
Boiling Point	100 °C
Specific Heat	4180 J/kg per °C
Latent Heat	333.55 kJ/kg
Viscosity	893.5 x 10^{-6} kg-s/m
pH	approximately 7.0

2. Carbon Nanotubes

The single-wall and hollow, multi-wall CNTs used in this study were purchased from Nano-Lab Incorporated located in Newton, Massachusetts. The CNTs were synthesized by the chemical-vapor deposition processing technique. CNTs with a high aspect ratio, or length to diameter ratio, were selected for this study. Residual impurities from the synthesis process include less than 1% weight of iron and sulfur [21]. Table 3 lists the Nano-Lab CNT characteristics.

Table 3. Nano-Lab Incorporated CNT Characteristics

CNT Type	Structure	Catalog Number	Length (µm)	Diameter (nm)	Purity
MWCNT	Hollow	PD15L520	5 - 20	15 +/- 5	> 95%
SWCNT	-	D1L110	1 - 10	1	> 80%

In support of this study, prepared and processed CNT-enhanced nanofluids were provided by Luna Innovations Incorporated located in Danville, Virginia. All nanofluids were SWCNT-based with two purity levels and three CNT concentration levels. The CNT synthesis and dispersion techniques used by Luna Innovations are unknown. Their purity classification relied upon the Haddon method where purification levels above 100% were achieved by oxidation and nitric acid treatments. The CNTs were ultrasonically dispersed in distilled water using a 2.0% volumetric loading of gum Arabic surfactant [17]. Table 4 is a summary chart of the nanofluids prepared by Luna Innovations.

Table 4. Luna Innovations Incorporated Nanofluid Information

Sample	CNT Loading % (vol)	Purity %
LnW - 0402	0.05	117.0
LnW - 0403	0.1	117.0
LnW - 0404	0.2	117.0
LnW - 0405	0.05	144.0
LnW - 0406	0.1	144.0
LnW - 0407	0.2	144.0

3. Volumetric Loading Percentages

Based on the results of previous research, the NPS research experimental values, and the concentration of the Luna Innovations nanofluids, CNT loadings for this study were selected to be 0.1% and 0.2% volume. The surfactant loading was fixed at 3.0% volume to reduce the number of samples that could be reasonably evaluated within the scope of this study.

4. Surfactants

Chemical dispersion of the CNTs was accomplished by using Lithium Dodecyl Sulfate (LDS) (anionic) and Igepal CO-630 (non-ionic) surfactants manufactured by Sigma-Aldrich. These compounds were selected based on previous NPS research and to evaluate their effects on nanofluid electrical resistance measurements. Both LDS and Igepal are soluble in water, where LDS is in the form of a white-powder and Igepal is a clear, viscous liquid compound. Detailed information on the surfactants can be found in reference [22].

C. EQUIPMENT DESCRIPTION

Physical dispersion was accomplished by using a mechanical homogenizer and ultrasonicator. An industrial freezer unit was used to enable the liquid-to-solid phase change of the nanofluid. All electrical resistance measurements were taken using a digital multimeter. The following sections describe the details of the equipment used in this study.

1. Mechanical Homogenizer

A Stir-Pak mechanical homogenizer (stirrer) manufactured by Cole-Parmer Instrument Company was used to homogenize the surfactant and the CNT additions into the distilled water. A single propeller attachment was used during the homogenization process. The homogenizer did not have an isolation assembly to prevent atmospheric gasses from dissolving into the nanofluid during homogenization. Figure 3 shows a photograph of the homogenizer.

2. Ultrasonicator

A Sonicator 3000 Ultrasonic Liquid Processor manufactured by Misonix Incorporated was used for CNT dispersion. The ultrasonicator comprised of a probe tip that transmitted ultrasonic energy into the nanofluid. The available ultrasonication power settings were from 6 Watts to 42 Watts in 3 Watt increments with no alternate output power setting available. A temperature probe was used to monitor the temperature of the nanofluid during ultrasonication. Figure 3 shows a photograph of the ultrasonicator.

Figure 3. (Left) Stir-Pak Mechanical Stirrer. (Right) Sonicator 3000 Ultrasonic Liquid Processor

3. Commercial Freezer Unit

A commercial deep freezer unit manufactured by Westinghouse was used to conduct the liquid-to-solid phase change of the nanofluid. The freezer unit was set at a constant temperature of -13°C. Figure 4 is a photograph of the freezer unit.

Figure 4. Westinghouse Commercial Freezer Unit

4. Digital Multimeter

An 8840A digital multimeter manufactured by Fluke Industries was used to measure the electrical resistance of the nanofluid. A two-wire setup was selected since the lead resistance was negligible when compared to the overall resistance of the nanofluid. Figure 5 is a photograph of the multimeter.

Figure 5. Fluke 8840A Digital Multimeter

D. EXPERIMENTAL PROCEDURES

The following procedure builds upon the nanofluid preparation protocol developed by Kuhlmann [19]. The following steps outline the preparation procedure used in this study:

- 20 mL of distilled water was poured into a non-conductive, glass beaker.
- Surfactant was measured out and placed directly into the distilled water in accordance with the prescribed test matrix.
- The distilled water and surfactant mixture was homogenized at 600 RPM using the Stir-Pak with a single-propeller attachment. The attachment was placed approximately 0.25 inches from the bottom of the beaker to avoid cavitation and foaming at the surface. The mixture was homogenized until the surfactant was completely dissolved into the distilled water. This process took approximately five minutes for samples containing LDS and thirty minutes for samples containing Igepal.

- CNTs were measured out in accordance with the prescribed test matrix and added to the distilled water and surfactant mixture. The sample will now be referred to as a nanofluid.
- The nanofluid was homogenized at 600 RPM using the Stir-Pak with the same single propeller attachment for thirty minutes.
- The nanofluid was ultrasonicated in accordance with the prescribed test matrix. The ultrasonicator probe was placed approximately 0.25 inches from the bottom of the beaker to avoid foaming in the nanofluid. The temperature of the nanofluid was monitored through the duration of ultrasonication.

  Due to boiling of the nanofluid during ultrasonication, various ultrasonication power settings and time duration were selected. It should be noted that ultrasonication parameters varied in order to produce a well homogenized, stable nanofluid and *were not optimized for this study.*
- The initial resistance measurements were taken after the nanofluid cooled at room temperature for five minutes.
- All instruments were cleaned using only distilled water. The procedure was repeated for the next sample.

The American Society of Testing and Materials (ASTM) International document D1125—95, Standard Test Methods for Electrical Conductivity and Resistivity of Water, outlines the standard procedures that should be used for static (non-flowing) and continuous in-line conductivity and resistivity measurements. For this study, conductivity measurements could not be taken in strict adherence with the ASTM procedure due to the lack of available testing apparatus described by the ASTM. For detailed information on the ASTM measurement procedures see reference [23].

The nanofluids received from Luna Innovations Inc. were not modified for this study. All samples were taken directly from the container in which they arrived in from Luna Innovations.

Due to the potential health hazards that CNTs pose to the user, basic safety precautions were followed. Nitrile gloves, a protective face mask and safety glasses were used when handling CNTs and the nanofluids. All nanofluids were prepared inside a fume hood that was vented to the atmosphere. All waste and contaminated CNT-enhanced fluids were disposed of using a hazardous material storage tank.

E. EXPERIMENTAL VALIDATION

The success of this study hinged upon the ability to effectively reduce the influence of physical phenomena on the electrical resistance of the nanofluid. Through the initial testing process, this study expected to show a trend that the addition of CNTs does improve the electrical conductivity of the base fluid by decreasing the overall electrical resistance. The results of the initial testing revealed that the most significant factor affecting the electrical resistance measurements of the nanofluid proved to be the construction of the testing assembly.

The initial test assembly consisted of two, 3000 series aluminum plates separated by a 0.5mm thick, non-conducting plastic insulator. The assembly was sealed with waterproof, silicone caulk and multiple, electrically insulated spring clamps placed around the perimeter of the assembly. A nanofluid with concentration of 3.0% Igepal and 0.5% (weight) Bamboo-type, MWCNTs was injected into the assembly using a syringe through a fill-hole drilled in the upper plate sealed with a cork stopper. A smaller hole was also drilled in the upper plate to allow air to escape during the fill process. A direct current (DC) resistance measurement was taken by placing the multimeter leads on the upper and lower plate. An alternating current (AC) voltage measurement using a low voltage signal generator and known resistance in series with the plate assembly was used to calculate the assembly resistance. The DC resistance measurements were compared to the calculated AC resistances to assess any variation due to the test assembly. Resistance measurements of only the distilled water; distilled water and surfactant; and distilled water, surfactant and CNTs were recorded to evaluate the effects each had on the resistance of the base fluid. Figure 6 shows a photograph of the plate assembly.

Since the construction of the test assembly closely resembled that of a capacitor, a capacitive reactance and sensitivity to both polarity and frequency existed within the assembly. This resulted in an unsteady and indefinite resistance measurement. Also, achieving an adequate dispersion of the nanofluid within the plate assembly was hindered due to the small dimensions of the channel between the upper and lower plate. These phenomena and physical variables prevented clear-cut measurements along with the

inability to accurately correlate the calculated AC resistance to the DC resistance measurement. Figure 6 shows the inadequate dispersion of the nanofluid within the plate assembly.

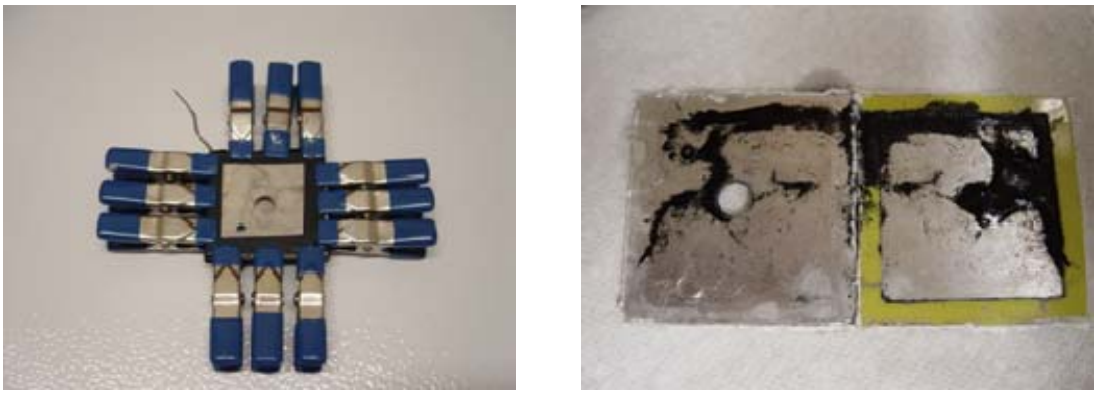

Figure 6. (Left) Aluminum Plate Assembly. (Right) Inadequate Dispersion of the Nanofluid within the Plate Assembly.

The suspected trend that CNTs would improve the electrical conductivity of a base fluid was shown through the initial testing. For example, the calculated AC resistance of the distilled water ranged between 3,100 Ω and 3,400 Ω compared to 645 Ω to 675 Ω with the distilled water and surfactant and finally 520 Ω to 575 Ω with the nanofluid. Since the calculated resistance values of distilled water did not approximately equal the accepted distilled water resistance value of 18.18 MΩ-cm [24] along with inconsistent resistance values, the plate assembly was suspect of error. Figure 7 shows the trend of decreasing resistance through the addition of surfactant and CNTs to the distilled water. Appendix A shows the plate assembly initial resistance measurements.

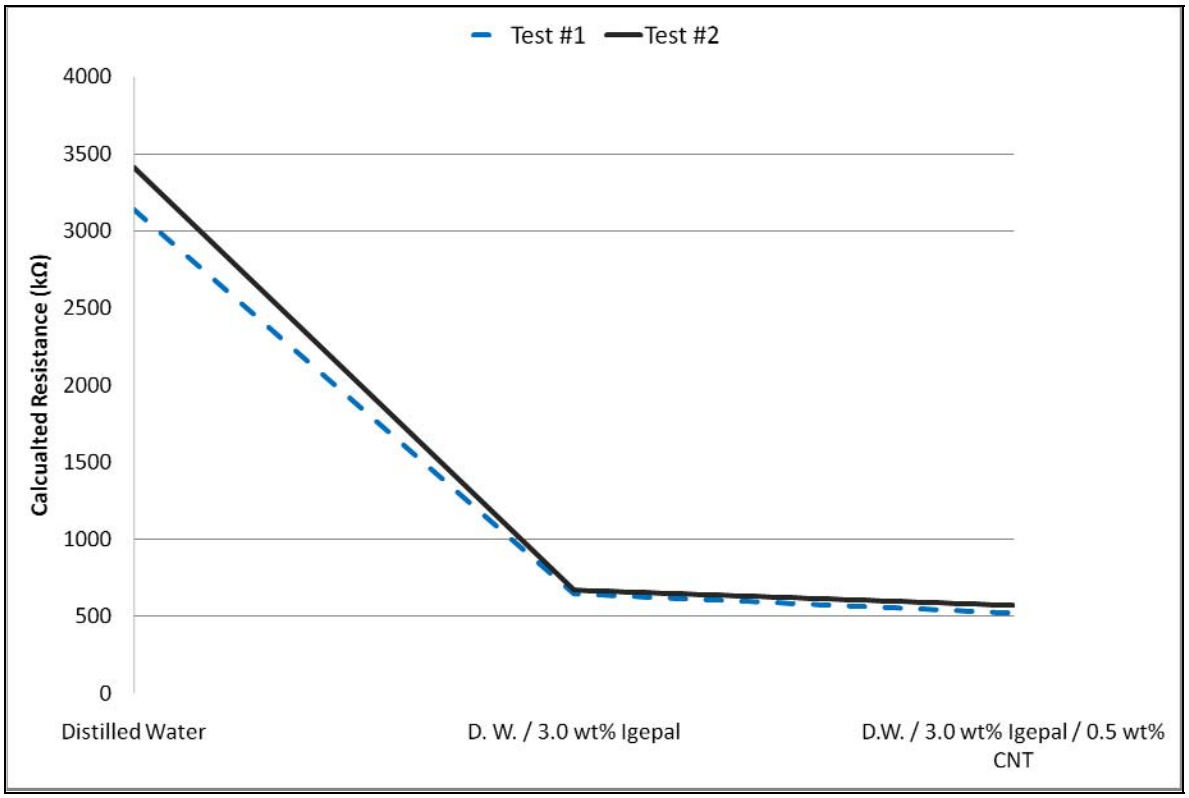

Figure 7. Initial Electrical Conductivity Trend using the Plate Assembly

In order to minimize error or variation introduced by the plate assembly construction, measurement setup, lead placement, contact resistance or nanofluid dispersion, a simplified probe-type test assembly was constructed. This assembly consisted of three, 0.125 inch diameter stainless steel rods, or probes, mounted in a non-conducting, plastic stopper. Each probe was labeled A, B, and C and were spaced 10mm apart. The probes were secured to the stopper so that the probe tips were in-line at 0.25 inches from the bottom of the beaker, but also able to be removed when taking resistance measurements. The multimeter leads were fastened to the probe using Fluke spring clips. DC Resistance measurements were taken between the A—B, B—C and A—C probes to measure the electrical resistance and to see if the resistance changed between various points in the nanofluid. Using the probe assembly, the intention was to show the same conductivity trend as seen with the plate assembly with minimal variation between measurements. Figure 8 is a photograph of the probe assembly.

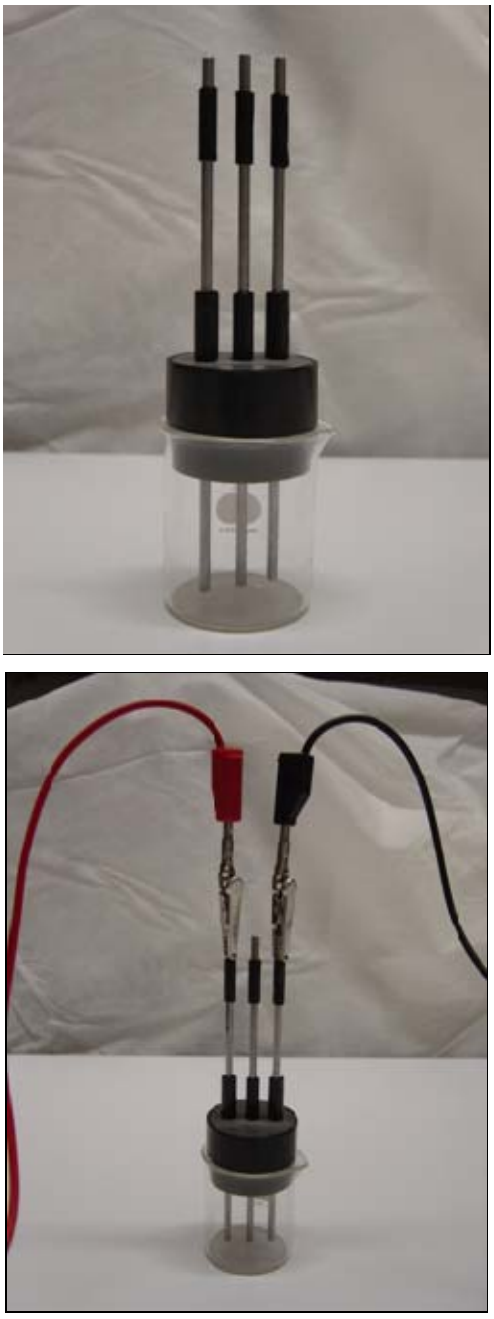

Figure 8. (Top) Probe Assembly. (Bottom) Probe Assembly with Leads

The following nanofluids were used in validating this test assembly:

- All Luna Innovations Nanofluids
- 0.5% (weight) Hollow-MWCNT with 3.0% (weight) Igepal
- 0.5% (weight) Bamboo-MWCNT with 3.0% (weight) Igepal

Resistance measurements between probes were conducted for a period of ten seconds. The beginning resistance value was recorded at the initial connection of the lead to the probe and the ending resistance value was recorded at the expiration of ten seconds. Probes not in use during the measurement were removed from the assembly.

Using the probe assembly, the second phase of experimental validation began with the thermal cycling of the nanofluid. After the initial resistance measurements were recorded, the nanofluid was placed in the deep freezer until completion of the liquid-to-solid phase change. The nanofluid was then removed from the freezer and thawed at room temperature until the completion of the solid-to-liquid phase change. The electrical resistance of the nanofluid was measured and recorded with additional notes on the physical appearance of the nanofluid, i.e., formation of agglomerates, layered separation of the CNTs from the distilled water, sedimentation of CNTs out of solution, etc. All nanofluids underwent five thermal cycles or until the sample showed signs of instability.

The initial results using the probe assembly showed the same trend of decreasing resistance with the addition of surfactant and CNTs but with significantly higher resistance ranges in excess of 30 kΩ compared to values of less than 1 kΩ using the plate assembly. Sporadic resistance readings of less than 10 kΩ made the probe assembly suspect to error. A possible reason for the large difference in resistance ranges could possibly be attributed to the small contact area between the teeth of the spring clip. If the clips did not make good contact or any contact at all with the probes, the contact resistance would significantly increase and prevent accurate measurements.

The physical stability of the nanofluids varied drastically between the Luna Innovation and NPS nanofluids. All of the Luna Innovation nanofluids showed excellent stability with minimal agglomeration and sedimentation after five phase changes. On the other hand, the NPS nanofluids were unstable due to the formation of a large, single agglomerate after the first thaw cycle. These initial results showed the sensitivity of nanofluids to the preparation procedure, loading concentrations and shows the need for nanofluid optimization. Figure 9 shows the physical appearance of the nanofluids upon completion of initial thermal cycling.

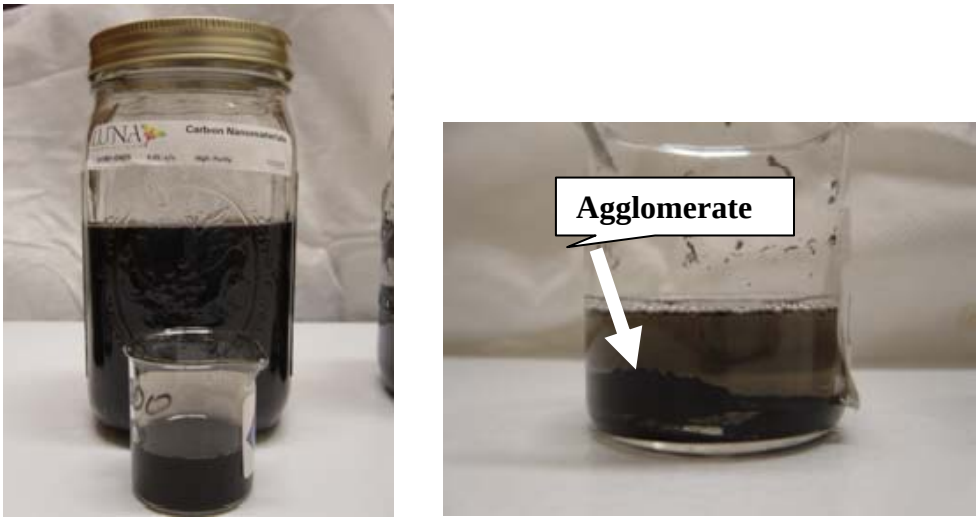

Figure 9. (Left) Luna Innovation LnW-404 Nanofluid after Five Phase Changes. (Right) NPS Nanofluid after One Phase Change

These initial results proved that the probe assembly needed to be further refined in order to achieve an accurate resistance measurement and that a lower CNT concentration needed to be selected to prevent the formation of agglomerates. To have comparable nanofluids, 0.2% and 0.1% volume CNT concentration were selected for NPS nanofluids. Appendices B, C and D show the raw electrical resistance data from the Luna Innovations, Hollow and Babmoo MWCNT nanofluids respectively.

The final test assembly was constructed using only the multimeter leads. This setup removed any variation introduced through the construction of a test assembly. The leads were fastened together using electrical tape with a 10mm distance between leads. The multimeter lead resistance was less than 1Ω and considered negligible when compared to the overall nanofluid resistance. A total of 15 resistance measurements were recorded to evaluate the variation between measurements and obtain a standard deviation between data points. Figure 10 shows a photograph of the multimeter lead construction.

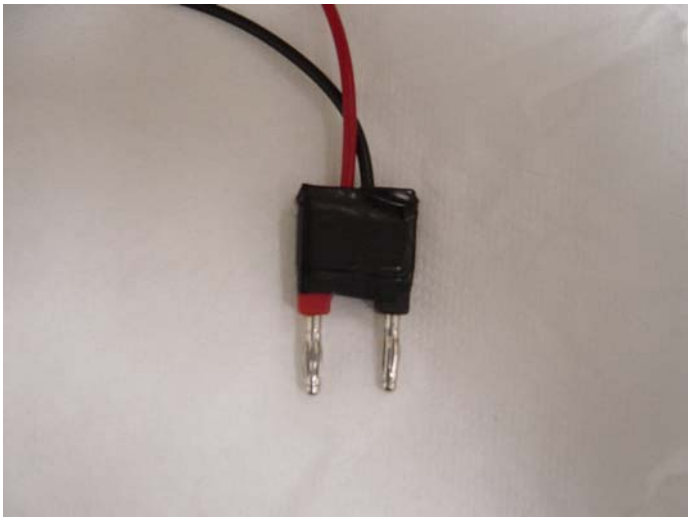

Figure 10. Multimeter Lead Construction

To determine the proper submersion depth of the leads, resistance measurements of all the Luna Innovations nanofluids were taken at the nanofluid surface and bottom of the beaker. Based on the results, the electrical resistance at the nanofluid surface was higher than the bottom of the beaker. This is possibly due to sedimentation effects of static, nanofluids where the CNTs naturally settle out of solution to the bottom of the container creating a more conductive path. In order to avoid these extreme electrical resistance values, resistance measurements would be taken at the mid-level of the nanofluid. Figure 11 shows a plot of the nanofluid surface and bottom average resistance values with the standard deviation between measurements. Appendix E shows the raw data of the electrical resistance measurements.

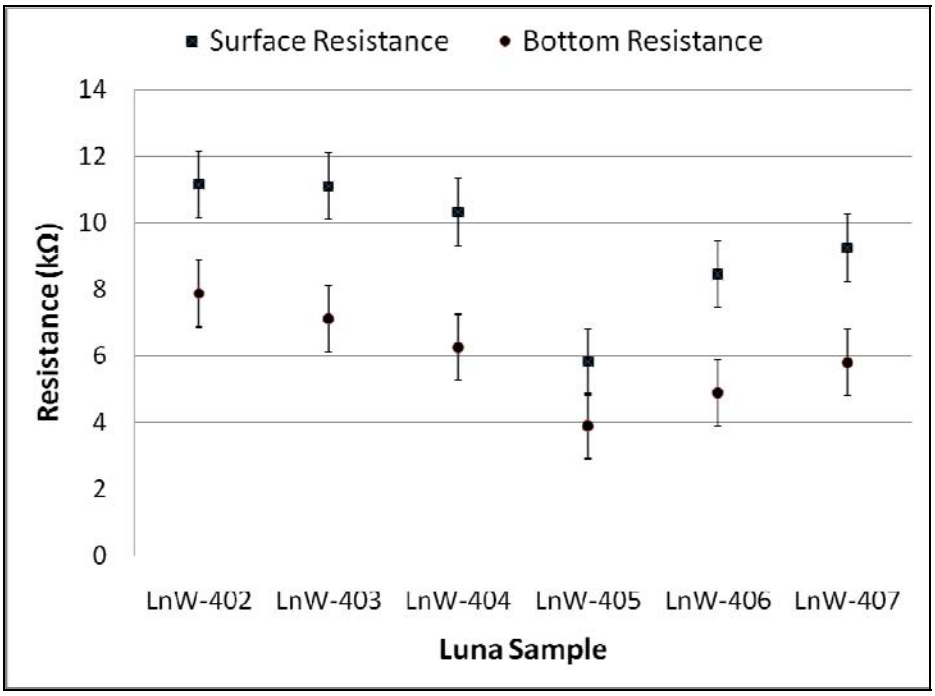

Figure 11. Luna Innovation Nanofluids Surface and Bottom Average Electrical Resistance Measurements.

The leads were rotated in 90° increments at the submerged mid-level in order to determine if the orientation of the leads affected the resistance measurements. Luna Innovation samples LnW-402 and LnW-405 were tested. The results showed less than a 3% difference between resistance measurements of different orientations. The orientation of the multimeter leads was considered negligible for the remainder of this study. Appendix F shows the raw data from the multimeter lead orientation measurements.

After establishing the submerged depth and orientation of the multimeter leads, all Luna Innovation nanofluids were tested and thermally cycled five times using new samples. The initial resistance measurement displayed on the multimeter screen at the moment of lead insertion was recorded. The results using this technique were the most promising of all the tests conducted. Not only did the nanofluids show excellent physical stability, but the resistance measurements ranged between 3 kΩ and 13 kΩ compared to readings in excess of 30 kΩ using the probe assembly.

1. Ultrasonication Parameter Validation

In order to determine the effects of ultrasonication during the preparation process of the nanofluid, four different power settings and time durations were evaluated using distilled water with a 3.0% (volume) concentration of LDS and Igepal surfactants. Table 5 lists the tested ultrasonication settings.

Table 5. Ultrasonication Power Settings and Time Durations

Power (Watts)	Time (Minutes)
39	5
24	30
15	15
15	60

The largest problem encountered during ultrasonication was controlling the mixture temperature. The energy input from the ultrasonicator caused an increase in mixture temperature, which resulted in excessive foaming, boiling and evaporation of liquid. This significantly altered the volume concentration of surfactant in the mixture. 4mL to 7mL of liquid evaporated when the mixture was ultrasonicated at 24 Watts for 30 minutes and 15 Watts for 60 minutes. Less than 1ml of liquid evaporated using an ultrasonication setting of 39 Watts for 5 minutes and 15 Watts for 15 minutes. In some cases, the mixtures containing Igepal turned an opaque color at temperatures above 40°C whereas the LDS mixtures did not.

In order to control the mixture temperature while ensuring an adequate homogenization of CNTs, using an ice bath during preparation or using the 15 Watts for 15 minutes setting with no ice bath (uncontrolled temperature) could be used. To ensure the preparation of a well homogenized, stable sample with minimal liquid loss, nanofluids were prepared using an ultrasonication setting of 15 Watts for 15 minutes both with and without an ice bath.

F. EXPERIMENTAL SUMMARY

Nanofluids prepared by NPS consisted of 0.1% (volume) and 0.2% (volume) concentrations of MWCNTs and SWCNTs dispersed in distilled water using a 3.0% (volume) concentration of LDS or Igepal surfactant. The nanofluids were prepared using a combination of physical and chemical means. Based on the results of the experimental validation, the DC electrical resistances of the nanofluids will be tested using only the multimeter leads submerged at mid-level at any orientation in the nanofluid. 15 resistance measurements were recorded from the initial insertion of the leads into the nanofluid and subsequent display on the multimeter screen. All nanofluids (except Luna Innovations samples) will be ultrasonicated at a power setting of 15 Watts for 15 minutes both with and without the use of an ice bath. The initial resistance measurements will be taken five minutes after the completion of ultrasonication. All samples will be thermally cycled up to five times or until the sample shows any signs of instability, in which testing will be discontinued. Table 6 lists the NPS Nanofluid Experimental Matrix and Table 4 lists the Luna Innovation Nanofluids that will be used for this study.

Table 6. NPS Nanofluid Experimental Matrix

Sample	Ultrasonication Temperature Control	CNT Type	CNT Concentration (% Volume)	Surfactant Concentration (3.0% Volume)
1	Ice Bath	MWCNT	0.2	LDS
2	Ice Bath	MWCNT	0.2	Igepal
3	Ice Bath	SWCNT	0.2	LDS
4	Ice Bath	SWCNT	0.2	Igepal
5	Ice Bath	MWCNT	0.1	LDS
6	Ice Bath	MWCNT	0.1	Igepal
7	Ice Bath	SWCNT	0.1	LDS
8	Ice Bath	SWCNT	0.1	Igepal
9	None	MWCNT	0.2	LDS
10	None	MWCNT	0.2	Igepal
11	None	SWCNT	0.2	LDS
12	None	SWCNT	0.2	Igepal
13	None	MWCNT	0.1	LDS
14	None	MWCNT	0.1	Igepal
15	None	SWCNT	0.1	LDS
16	None	SWCNT	0.1	Igepal

The Luna Innovations samples will be thermally cycled up to twelve times to evaluate the stability through extended thermal cycles and re-ultrasonicated at 15 Watts for five minutes to investigate the need for re-homogenization of static, CNT-enhanced nanofluids. Resistance measurements will only be taken at the sixth and twelfth thermal cycles.

1. Ancillary Studies

Ancillary studies focused on the stability of the surfactant during thermal cycling and the effects of mixing of Luna Innovation nanofluids with Nano-Lab Industries. The selected surfactants, LDS and Igepal, were homogenized in 20 mL of distilled water and prepared using the ultrasonication settings listed in Table 7, both with and without an ice bath. All mixtures were thermally cycled three times to evaluate the overall stability during the initial phase changes.

Table 7. Experimental Matrix for Thermal Cycling of Surfactants

Surfactant	LDS & Igepal	LDS & Igepal	LDS & Igepal	LDS & Igepal
Concentration	3.0 % vol	3.0 % vol	3.0 % vol	3.0 % vol
Ultrasonication Power	39 W	24 W	15 W	15 W
Ultrasonication Time	5 min	30 min	15 min	60 min

For the mixing of different types of CNTs, Nano-Lab Industries hollow-type MWCNTs were mixed with Luna Innovations SWCNT nanofluids. 0.05% (volume) MWCNTs were added to LnW-402 and LnW-405 and ultrasonicated at 39 Watts for 5 minutes and 15 Watts for 15 minutes both with and without and ice bath. The combined CNT concentration of 0.1% (volume) was compared to the LnW-403 and LnW-406 to evaluate their effects on the nanofluid resistance. The ultrasonication settings were selected in order to minimize liquid evaporation during ultrasonication. The nanofluids will be thermally cycled up to five times or until the nanofluid shows signs of instability. Table 8 lists the combined CNT nanofluid experimental matrix.

Table 8. Combined CNT Nanofluid Experimental Matrix

Sample	Luna Innovation Nanofluid	Nano-Lab CNT	Ice Bath during Ultrasonication (Yes / No)	Ultrasonication Power (Watts)	Ultrasonication Time (Minutes)
L1	LnW-402	0.05% volume Hollow MWCNT	Yes	15	15
L2			No	15	15
L3			Yes	39	5
L4			No	39	5
L5	LnW-405	0.05% volume Hollow MWCNT	Yes	15	15
L6			No	15	15
L7			Yes	39	5
L8			No	39	5

THIS PAGE INTENTIONALLY LEFT BLANK

III. RESULTS

The results of this study are presented in a tabular format on the following pages. Each table lists the average DC resistance of 15 resistance measurements using only the multimeter leads. A transparency test was conducted upon the completion of the solid-to-liquid phase change, where the nanofluid was tilted on-edge against white, ambient light and evaluated for the existence of sediment or agglomerates. Table 9 identifies the terms assigned to describe the physical appearance of the nanofluids and Figure 12 is a photograph of the respective terms. Tables 10 through 13 summarize the average resistance measurements of the NPS nanofluids, Luna Innovations nanofluids, combined CNT nanofluids and thermal cycling of surfactant tests respectively. All electrical resistance measurements can be found in Appendices G, H, and I respectively.

Table 9. Description of Physical Appearance of Nanofluid

C	Clear
H	Homogenous
VSA	Very Small Agglomerates
SA	Small Agglomerates
MA	Medium Agglomerates
LA	Large Agglomerates
LS	Light Sediment
S	Sediment
HS	Heavy Sediment

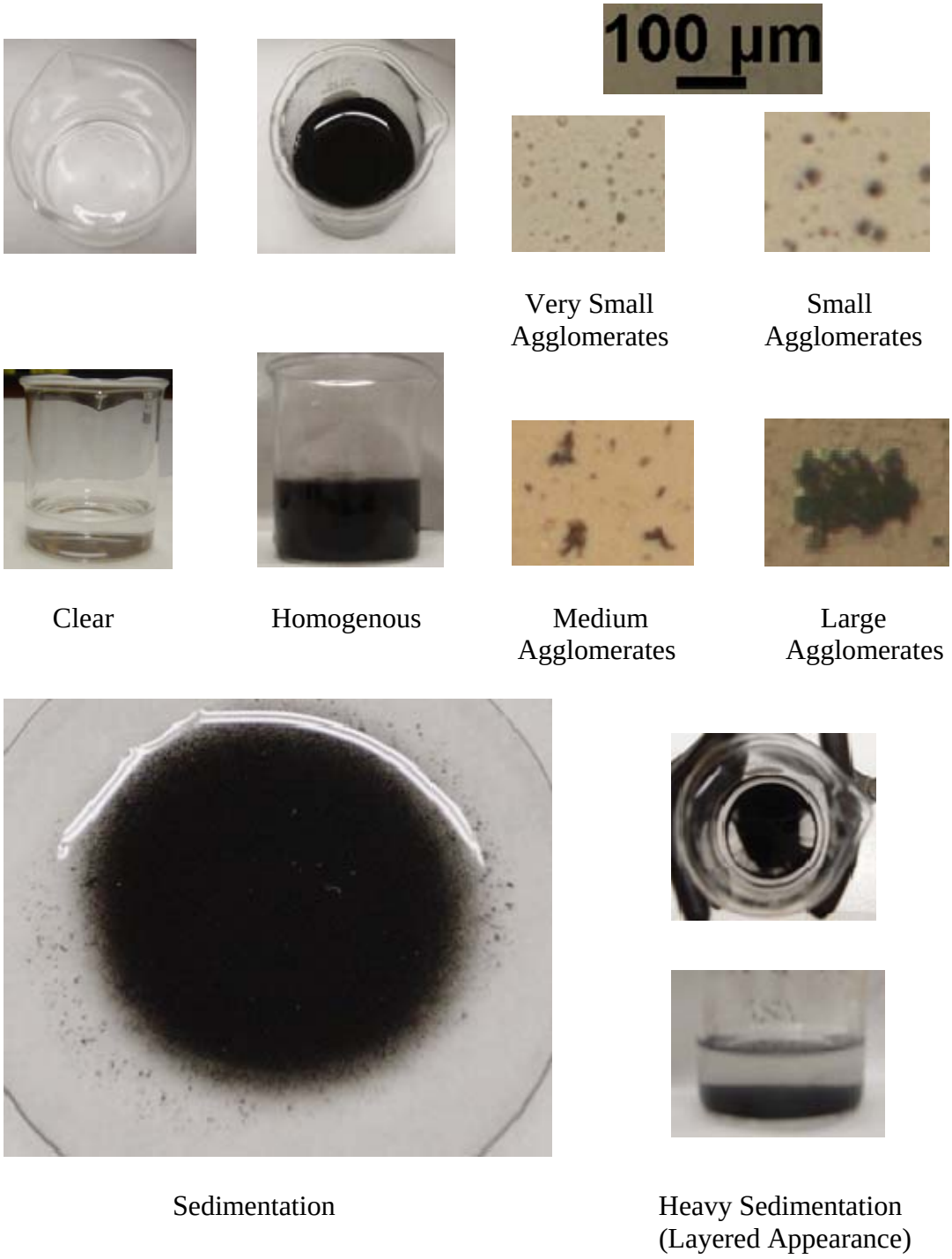

Figure 12. Photographs Describing Physical Appearance of Nanofluids

Table 10. NPS Nanofluid Results

			Average Resistance (kΩ)						
Sample	**Type of Surfactant**	**DW (MΩ)**	**DW / LDS**	**Initial**	**1st Thaw**	**2nd Thaw**	**3rd Thaw**	**4th Thaw**	**5th Thaw**
1	LDS	0.34	13.47	12.24	8.53	8.43	6.97	6.73	7.13
	Appearance	C	C	H	LS	SA & S	SA & S	SA & S	SA & S
2	Igepal	0.19	38.95	37.71	30.36	31.25	30.26	30.97	26.43
	Appearance	C	C	H	LS	SA & S	SA & S	MA & S	MA, LA & S
3	LDS	0.23	13.62	6.01	8.69	10.21	8.26	8.25	7.26
	Appearance	C	C	H	LS	LS	SA & S	SA & S	SA & S
4	Igepal	0.24	34.86	36.43	30.57	30.21	28.97	-	-
	Appearance	C	C	H	LS	LS	Unstable - Layered Apperance		
5	LDS	0.28	14.96	9.65	8.07	9.85	10.18	8.69	7.17
	Appearance	C	C	H	SA	SA	SA	SA & MA	LA
6	Igepal	0.24	35.23	36.53	30.18	28.03	30.54	24.7	24.69
	Appearance	C	C	H	LS	VSA	VSA	VSA	VSA
7	LDS	0.22	13.54	5.58	12.15	12.02	10.35	9.19	8.73
	Appearance	C	C	H	LS	LS	LS	LS	LS
8	Igepal	0.26	34.59	40.56	31.07	29.11	25.76	-	-
	Appearance	C	C	H	LS	HS	Unstable - Layered Appearance		
9	LDS	0.71	9.87	2.55	8.23	7.53	5.77	8.36	5.17
	Appearance	C	C	H	SA	SA	MA	MA	MA
10	Igepal	0.68	37.29	15.58	29.61	30.24	24.91	27.38	27.55
	Appearance	C	C	H	SA	SA & S	LA & S	LA & S	LA & S
11	LDS	0.71	12.01	3.48	8.98	8.07	8.17	8.19	8.41
	Appearance	C	C	H	LS	LS	LS	LS	LS
12	Igepal	0.52	31.41	-	-	-	-	-	-
	Appearance	C	C	Unstable - Layered Separation after Ultrasonication					
13	LDS	0.62	8.97	4.62	8.36	8.17	7.18	7.89	9.99
	Appearance	C	C	H	SA	SA	SA	SA	SA
14	Igepal	0.65	32.55	12.03	29.64	25.55	25.73	30.79	31.26
	Appearance	C	C	H	VSA	SA	SA	SA	SA
15	LDS	0.56	8.85	5.55	9.46	8.97	9.19	6.61	8.08
	Appearance	C	C	H	LS	LS	LS	LS	LS
16	Igepal	0.61	29.53	-	-	-	-	-	-
	Appearance	C	C	Unstable - Layered Separation after Ultrasonication					

Table 11. Luna Innovations Incorporated Nanofluid Results

		Average Resistance (kΩ)									
Sample	**Type of Surfactant**	**Initial**	**1st Thaw**	**2nd Thaw**	**3rd Thaw**	**4th Thaw**	**5th Thaw**	**6th Thaw**	**12th Thaw**	**Re-Sonicate**	**1st Thaw**
LnW-402	Gum Arabic	10.73	11.91	12.82	12.12	12.7	8.77	9.97	21.55	7.73	11.84
	Appearance	H	H	H	H	H	H	SA	LA & S	H	SA
LnW-403	Gum Arabic	8.58	11.3	11.55	11.41	12.3	9.13	9.78	20.54	6.94	11.23
	Appearance	H	H	H	H	H	H	SA	LA & S	H	SA
LnW-404	Gum Arabic	7.82	9.05	8.92	8.85	8.27	8.53	8.81	17.9	6.71	7.23
	Appearance	H	H	H	H	H	H	LS	MA & S	H	SA
LnW-405	Gum Arabic	4.69	6.68	7.31	7.28	6.3	5.1	6.35	13.16	6.47	9.91
	Appearance	H	H	H	H	H	H	SA	MA & S	H	SA
LnW-406	Gum Arabic	6.47	9.44	8.45	8.77	7.55	6.76	7.45	12.37	7.34	9.49
	Appearance	H	H	H	H	H	H	S	MA & S	H	SA
LnW-407	Gum Arabic	7.4	10.14	9.05	9.77	8.22	7.28	7.99	16.41	6.9	9.63
	Appearance	H	H	H	H	H	H	LS	MA	H	SA

Table 12. Combined CNT Nanofluid Results

			Average Resistance (kΩ)					
Sample	**Luna Innovation Nanofluid**	**Luna Innovation**	**Mixed CNT Initial**	**1st Thaw**	**2nd Thaw**	**3rd Thaw**	**4th Thaw**	**5th Thaw**
L1	Gum Arabic	8.47	7.94	16.51	7.95	10.35	14.45	17.15
	Appearance	H	H	S	Unstable - HA and Layered Appearance			
L2	Gum Arabic	8.43	6.01	16.98	9.05	11.93	12.01	16.81
	Appearance	H	H	S	SA & S	SA & S	SA & S	SA & S
L3	Gum Arabic	8.66	7.32	16.83	9.09	13.41	17.05	18.73
	Appearance	H	H	S	Unstable - HA and Layered Appearance			
L4	Gum Arabic	8.11	5.53	18.1	8.81	11.59	17.58	18.99
	Appearance	H	H	Unstable - HA & S				
L5	Gum Arabic	7.86	7.33	9.55	11.93	11.27	-	-
	Appearance	H	H	S	Unstable - HA and Layered Appearance			
L6	Gum Arabic	8.27	4.03	9.07	11.15	9.66	-	-
	Appearance	H	H	S	Unstable - HA and Layered Appearance			
L7	Gum Arabic	7.67	6.1	8.04	10.16	8.95	-	-
	Appearance	H	H	S	Unstable - HA and Layered Appearance			
L8	Gum Arabic	7.36	5.76	8.43	8.85	9.35	-	-
	Appearance	H	H	Unstable - HS & HA, Layered Appearance				

Table 13. Thermal Cycling of Surfactant Results

Surfactant		LDS using an Ice Bath					LDS (No Ice Bath)			
Loading		3.0% vol					3.0% vol			
Ultrasonication Power (Watts)		39	24	15	15		39	24	15	15
Ultrasonication Time (Minutes)		5	30	15	60		5	30	15	60
Average Resistance (kΩ)	Initial	13.84	9.93	13.45	8.48		10.35	5.09	10.55	3.67
	1st Thaw	13.17	9.85	13.74	9.25		13.34	11.32	12.21	-
	2nd Thaw	13.9	10.23	13.36	8.45		9.34	9.72	13.16	-
	3rd Thaw	15.66	12.61	14.87	9.01		15.06	12.1	13.33	-
Surfactant		Igepal using an Ice Bath					Igepal (No Ice Bath)			
Loading		3.0% vol					3.0% vol			
Ultrasonication Power (Watts)		39	24	15	15		39	24	15	15
Ultrasonication Time (Minutes)		5	30	15	60		5	30	15	60
Average Resistance (kΩ)	Initial	30.55	33.93	34.47	36.89		31.13	14.91	31.18	18.19
	1st Thaw	30.03	32.39	29.98	30.18		35.95	32.87	36.1	-
	2nd Thaw	39.79	37.34	38.11	38.11		42.93	36.71	40.05	-
	3rd Thaw	38.95	36.22	35.18	36.69		44.41	38.39	38.45	-

IV. ANALYSIS OF RESULTS

A. NPS NANOFLUIDS

Figure 13 is a plot of the average resistance throughout thermal cycling of all NPS samples. It shows a top-level view of the effects of ultrasonication temperature on the conductivity of the nanofluid and a conductivity comparison of nanofluids dispersed with either Igepal or LDS. Both SWCNT and MWCNT of all concentrations are displayed on the graph. Solid lines represent the nanofluids prepared using an ice bath during ultrasonication and the dashed lines represent nanofluids prepared without an ice bath during ultrasonication (uncontrolled temperature).

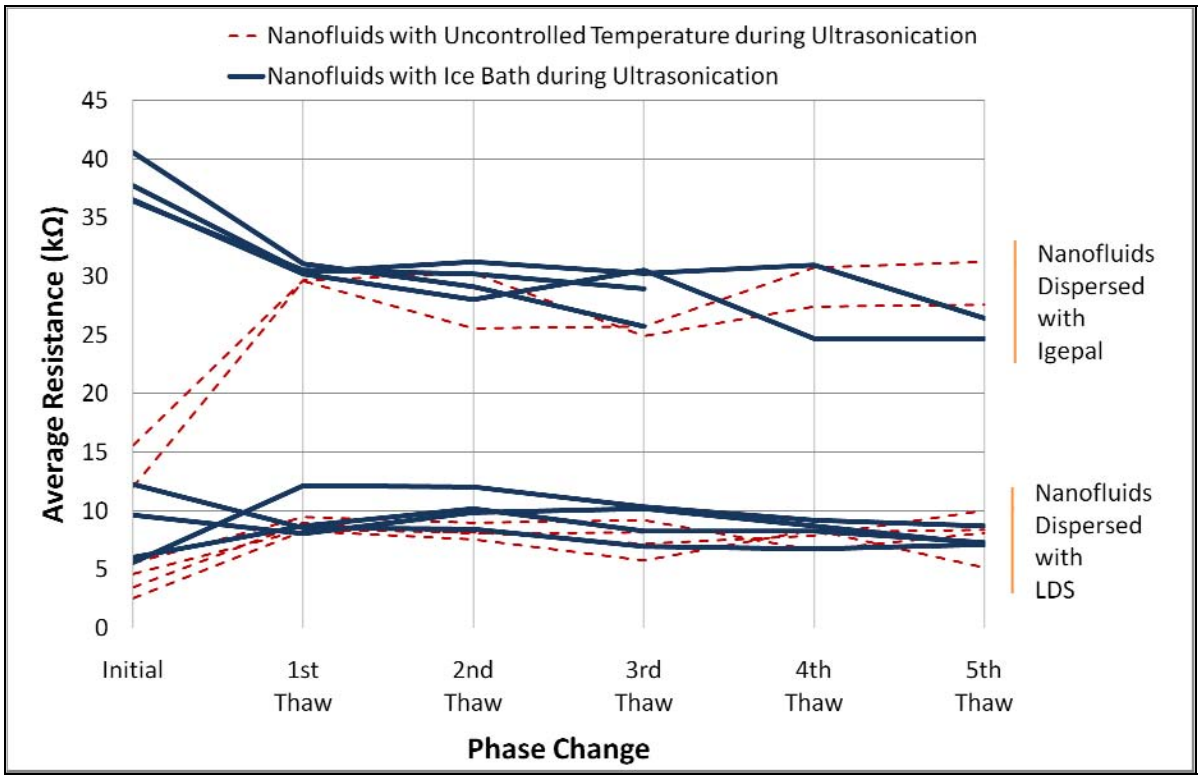

Figure 13. Average Resistance vs. Thermal Cycling of NPS Nanofluids

Using an ice bath during nanofluid ultrasonication did not have a significant effect on the nanofluid resistance throughout thermal cycling. All samples showed both increasing and decreasing changes in electrical resistance after the start of thermal cycling (1st Thaw). The largest difference in nanofluid resistance occurred at the initial

measurement due to the higher nanofluid temperatures at the time of measurement. Nanofluids prepared with no temperature control reached temperatures in excess of 70°C compared to 21°C using an ice bath. The conductivity of carbon is notably higher at warmer temperatures due to the increase in atomic movement within the lattice structure. This resulted in higher initial conductivities, or lower resistances, for samples ultrasonicated with no temperature control. After the first phase change, all nanofluids were at the same temperature, which resulted in a convergence of similar surfactant-based resistance measurements. Resistances both increased and decreased for the second through fifth phase changes. A decrease in resistance is possibly due to the natural sedimentation of CNTs out of solution, whereas, an increase in resistances is attributed to the breakdown of the CNT network and formation of agglomerates.

Nanofluids dispersed using LDS had lower resistances than those dispersed with Igepal. The conductive property of LDS assisted in the completion of the conductive paths within the CNT network, whereas the non-conductive property of Igepal was suspect of insulating adjacent CNTs or CNT networks. Also, nanofluids using LDS appeared to have less variation in average resistance values between phase changes than those using Igepal. The resistance values of all the LDS and Igepal samples after the final phase change were relatively the same showing that temperature control during ultrasonication does not have a significant impact on the conductivity of the nanofluid.

No apparent relationship between the effects of controlling nanofluid temperature during ultrasonication on the physical stability of the nanofluid could be identified. All samples showed signs of agglomeration or sedimentation, however, slightly larger agglomerates formed throughout the thermal cycling process in nanofluids using an ice bath.

Figure 14 and Figure 15 illustrate the effects that 0.1% and 0.2% concentration of MWCNTs and SWCNTs have on the resistance of the nanofluid. Each figure shows the average resistance of the nanofluid throughout thermal cycling. Nanofluids prepared both with and without an ice bath during ultrasonication are plotted in each figure.

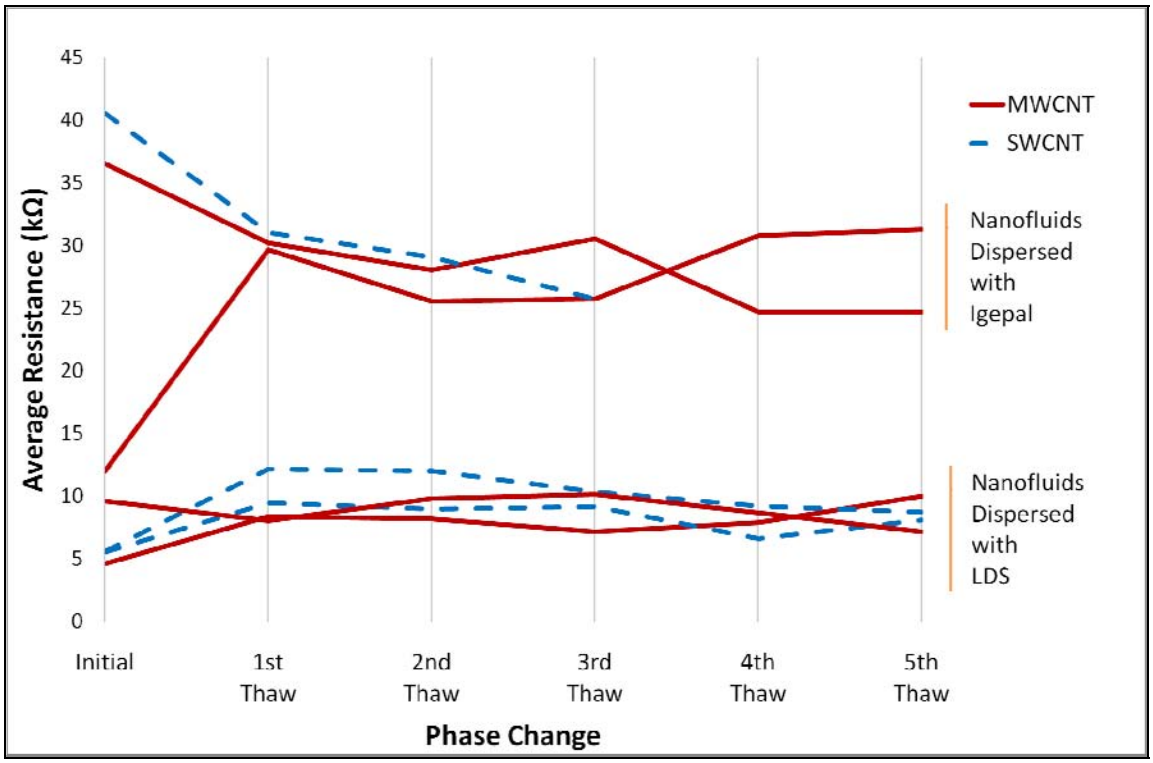

Figure 14. 0.1% CNT Loading: MWCNT & SWCNT Resistance Comparison

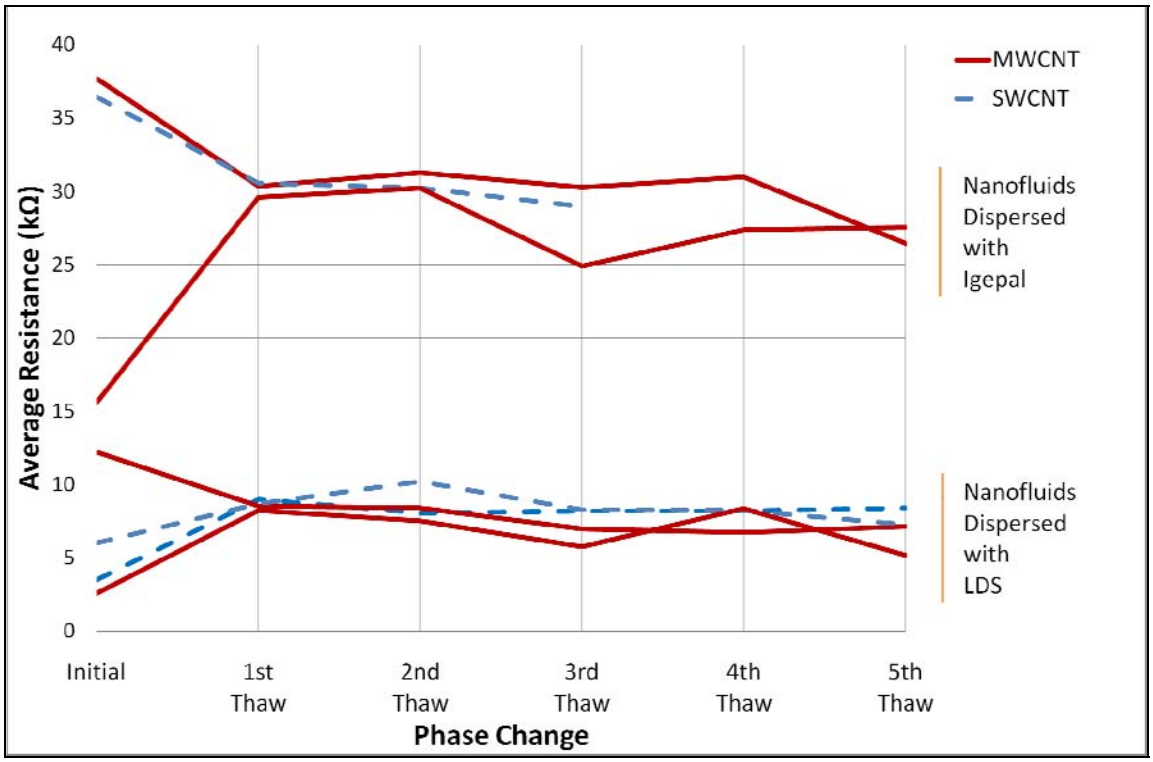

Figure 15. 0.2% CNT Loading: MWCNT & SWCNT Resistance Comparison

Based on the illustrated results in Figure 14 and Figure 15, the type of CNT does not significantly affect the resistance of the nanofluid. Neither MWCNTs nor SWCNTs dispersed in LDS or Igepal proved to show exceptional stability through thermal cycling. All samples using MWCNTs showed signs of agglomeration after the first phase change and SWCNTs showed signs of sedimentation as thermal cycling progressed. Neither type of CNT proved superior over the other within the respective concentration.

On the other hand, the concentration of CNTs had a minor impact on the resistance of the nanofluid. The 0.2% concentration of MWCNTs and SWCNTs showed a small decrease in the nanofluid resistance in both types of surfactants. However, larger-size agglomerates formed as thermal cycling progressed. Using higher concentrations of both SWCNTs and MWCNTs in LDS increased the conductivity of the respective nanofluids. Intuitively, this was expected since using more of a conducting material in a naturally conductive medium should increase the conductivity of the nanofluid. Further optimization of individual nanofluids should balance this trade-off between CNT concentration and acceptable agglomeration.

In both concentration cases, MWCNTs exhibited higher conductivities than SWCNTs. This result was unexpected since SWCNTs have a lower number of defects than MWCNTs, theoretically rendering a higher conductivity. Despite the conductivity gains with MWCNTs, the associated increase in agglomerate size during the progression of thermal cycling yielded those nanofluids more unstable than those using SWCNTs.

SWCNTs dispersed in Igepal showed to be more unstable than those dispersed in LDS. Igepal-based, SWCNT nanofluids prepared with an ice bath during ultrasonication were only stable until the third phase change, whereas, nanofluids using the same parameters were unable to be produced without using an ice bath during ultrasonication. These results should direct future research optimize individual nanofluid combinations.

B. LUNA INNOVATIONS INCORPORATED NANOFLUIDS

The Luna Innovations nanofluids showed exceptional stability throughout the first five thermal cycles. Light sedimentation and small agglomeration started after the sixth cycle followed by severe instability and agglomeration after the twelfth phase change. After the nanofluids were re-ultrasonicated, the resistances returned to a value near or lower than the initial resistance values. All nanofluids exhibited both increasing and decreasing average resistance values just as the NPS nanofluids. Under identical thermal cycling conditions, the similar trends displayed between each nanofluid may be due to the properties of the surfactant or characteristics of the CNTs selected by Luna Innovations. Figure 16 shows the physical breakdown of sample LnW-402 from initial testing, to the twelfth thermal cycle and appearance after re-sonication.

The nanofluids with a lower purity exhibited a decreasing resistance with higher CNT concentrations just as the NPS nanofluids, but the resistance of the higher purity samples increased as CNT concentration increased. No distinct conclusion could be drawn to explain this behavior. Figure 17 and Figure 18 show the average resistances throughout thermal cycling of the 117% and 144% pure nanofluids.

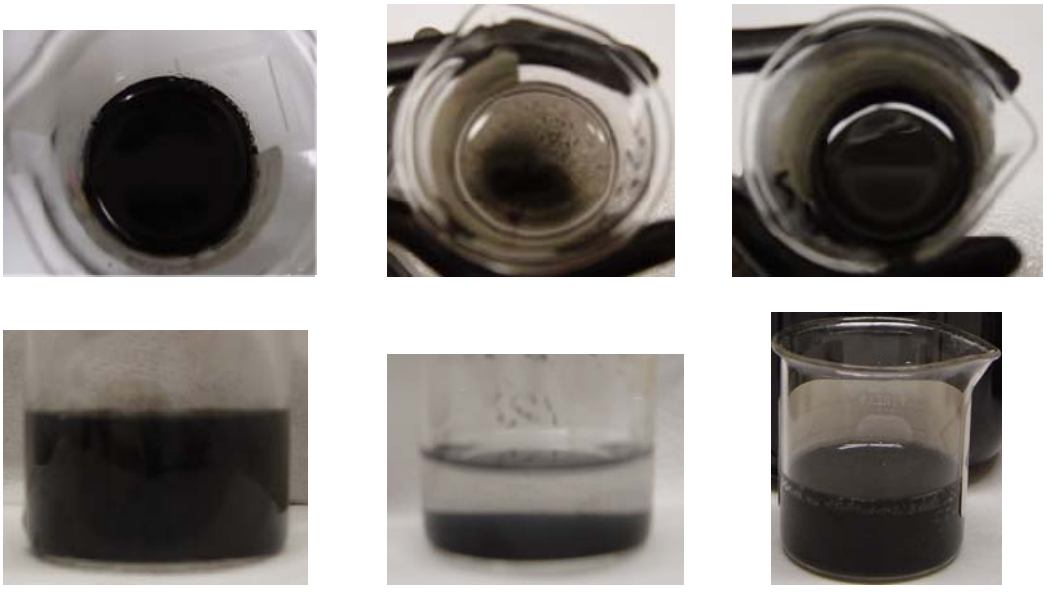

Figure 16. (Left) Initial Appearance of LnW-402. (Middle) Appearance of LnW-402 after 12th Cycle. (Right) Appearance of LnW-402 after Re-sonication

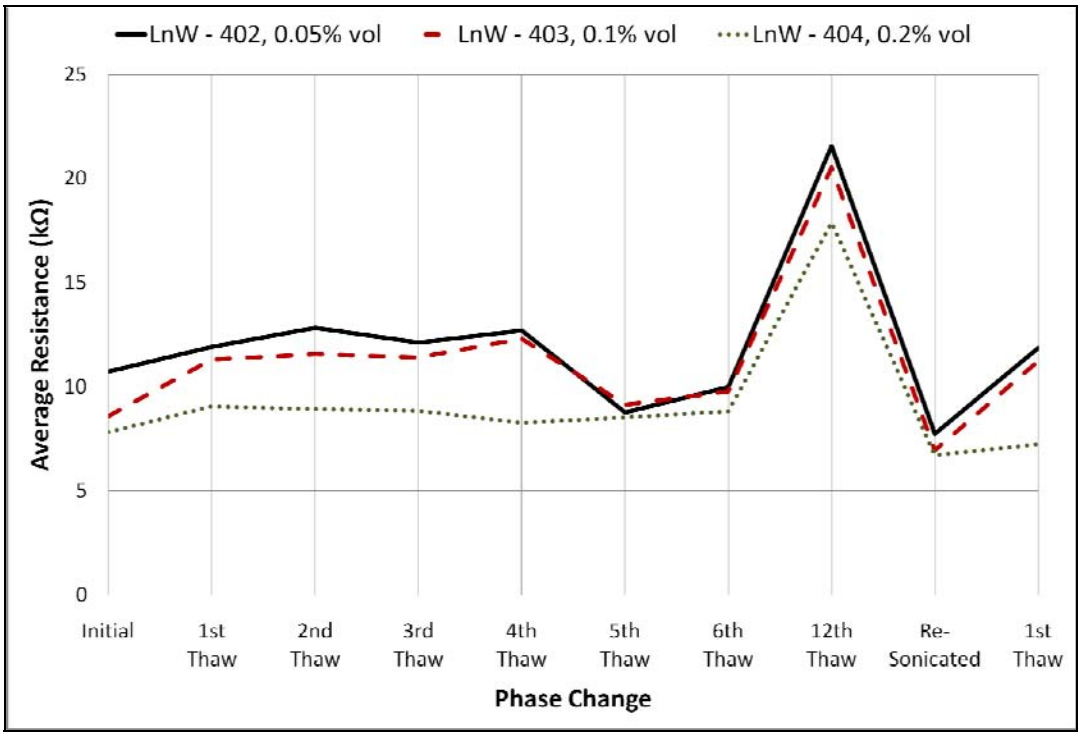

Figure 17. 117% Pure Luna Innovations Nanofluids

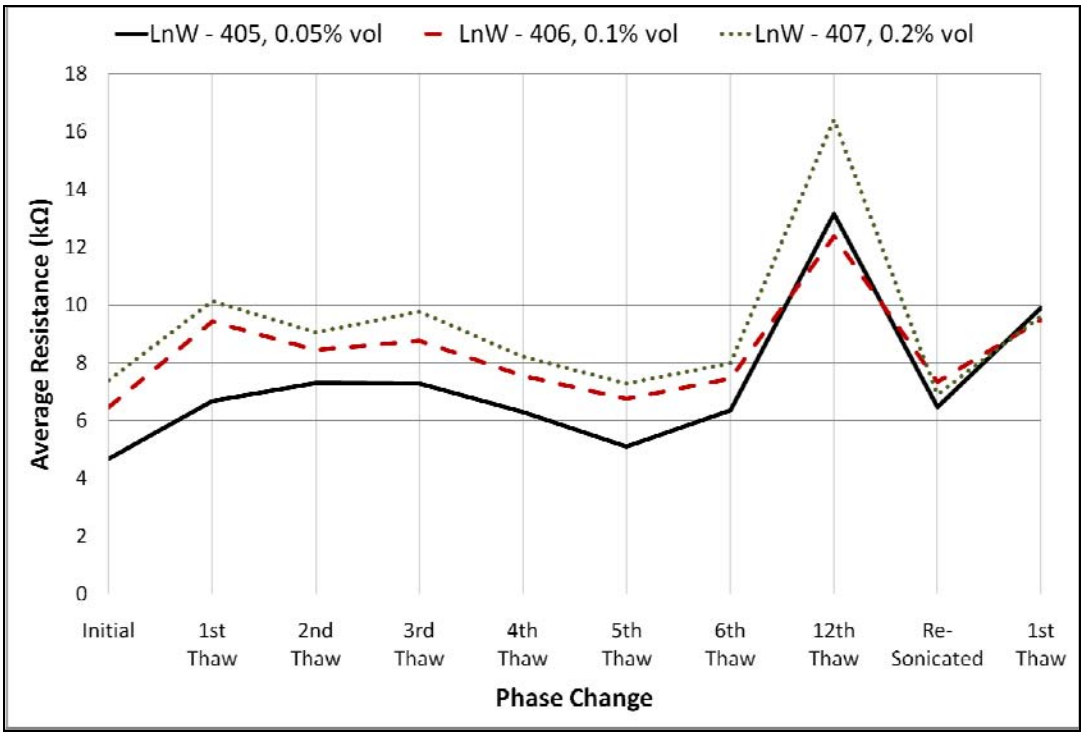

Figure 18. 144% Pure Luna Innovations Nanofluids

C. COMBINED CNT NANOFLUIDS

Combining the Nano-Lab MWCNTs with the Luna Innovations nanofluids did not have a significant effect on the resistance of the nanofluid. The initial measurement after ultrasonication was slightly less than the initial resistances of the 0.05% and 0.1% Luna nanofluid. Although this may seem beneficial, all mixed nanofluids were physically very unstable. In the lower purity samples, signs of agglomeration were noticed after the second phase change with increasing agglomerate formation in subsequent phase changes. The higher purity nanofluids were unstable after the first phase change exhibiting a layered appearance with heavy sedimentation and agglomerate formation.

This combination of CNTs and nanofluid showed to be unstable. However, this does not prove that combining various types of CNTs will always yield unstable nanofluids. Further investigation is required in this area of nanofluid technology.

D. SURFACTANT CYCLING

The average resistance of Igepal and LDS does slightly increase as thermal cycling progresses. The fluctuating trend during thermal cycling resembles the trend displayed by the NPS and Luna Innovations nanofluids. Regardless of the temperature control method used during ultrasonication, all surfactant mixtures maintained a homogenous distribution with no precipitation out of solution. The initial resistances of LDS and Igepal samples prepared without an ice bath were lower than those prepared with an ice bath due to the effects of heat generation during ultrasonication. Samples prepared without an ice bath that were ultrasonicated at 24 Watts for 30 minutes and 15 Watts for 60 minutes lost 4mL to 6mL of liquid due to evaporation. While the increasing resistance of the surfactants during thermal cycling may have a minor contribution to the increasing resistance trends of the nanofluids, it is not indicative of the effects on the heat transfer properties of the nanofluids. This study also shows the need for temperature control during preparation to prevent severely altered surfactant and CNT concentrations from the evaporation of liquid.

THIS PAGE INTENTIONALLY LEFT BLANK

V. CONCLUSION

Regardless of CNT type, size, concentration, preparation procedure, surfactant type, and surfactant concentration; those CNT-enhanced nanofluids used as a phase change material in this study were stable between three to five thermal cycles. Because both the electrical conductivity and thermal conductivity of a CNT-based nanofluid are dependent on maintaining a dispersed network of CNTs, the electrical conductivity tests proved a useful means of determining the breakdown of the CNT network during repeated phase changes. Increases in electrical resistance corresponded to observed agglomeration and sedimentation within the nanofluids. Although electrical conductivity testing does not provide thermal conductivity data directly, it can be used as a very practical means for monitoring a CNT-based nanofluid to ensure nanotubes are properly dispersed for enhanced thermal conductivity. In addition, repeated ultrasonication after CNT network breakdown (indicated by markedly increased electrical resistance) was shown to return resistances to values similar to those preceding breakdown. Thus, it may be possible to reagitate CNT nanofluids after breakdown to return them to their original state of dispersion. Electrical conductivity testing can be used to determine when such agitation is required, and when it has been satisfactorily accomplished. However, the trade-off between the addition of ultrasonication equipment and the reduction in cooling equipment size due to enhanced thermal conductivity must be addressed at the system level to determine whether it is advantageous.

In summary, this research has shown that CNT-based nanofluids can withstand a fair number of phase changes before significant agglomeration and sedimentation occur. The number of phase changes before such breakdown was dependent on the quality of initial nanofluid processing, but the nanofluids used in this study generally broke down in less than 12 cycles. Electrical conductivity testing should be considered as a means to monitor for such breakdown and determine when reagitation has been successful. Direct correlation between electrical and thermal conductivities is possible (although likely very dependent on nanofluid parameters), but was beyond the scope of this study.

THIS PAGE INTENTIONALLY LEFT BLANK

APPENDIX A. CALCULATED RESISTANCE VALUES USING THE PLATE ASSEMBLY

Test #1	**Distilled Water**	**D. W. 3.0 wt% Igepal**	**D.W. 3.0 wt% Igepal 0.5 wt% CNT**
Frequency (Hz)	10	10	10
Known Resistance - R_1 (Ω)	100,000	100,000	100,000
Input Voltage to Unknown Res - E_{R1}	1.020	1.007	1.17
AC Voltage Across Unknow Resistance - E - E_{R2} (V)	0.032	0.0065	0.0061
Calcualted Unknown Resistance - R_2 (Ω)	**3137.255**	**645.482**	**521.368**
DC Resistance Measurement (Ω) DC Reverse polarity Measurement (Ω)	- Unsteady, increase from 58 - 75 kohm - Somewhat unsteady, decrease from 72 - 64 kohm	- Unstable, 61 kohm decreasing to 45 kohm - Unstable, 53 kohm decreasing to 26 kohm	- Unstable, fluctuate between 36 - 40 kohm - Somewhat Stable between 8 10 kohm
Test #2	**Distilled Water**	**D. W. 3.0 wt% Igepal**	**D.W. 3.0 wt% Igepal 0.5 wt% CNT**
Frequency (Hz)	10	10	10
Known Resistance - R_1 (Ω)	100,000	100,000	100,000
Input Voltage to Unknown Res - E_{R1}	1.023	1.0106	1.0100
AC Voltage Across Unknow Resistance - E - E_{R2} (V)	0.0349	0.0068	0.0058
Calcualted Unknown Resistance - R_2 (Ω)	**3411.535**	**672.868**	**573.267**
DC Resistance Measurement (Ω) DC Reverse polarity Measurement (Ω)	- Somewhat Unsteady, 60 to 72 kohm - Unsteady, 79 to 45 kohm	- Unstable, 55 kohm decreasing to 38.6 kohm - Unstable, 40 kohm decreasing to 20 kohm	- Unstable, decreasing from 2.0 to less than 1.0 kohm - Unstable decrease from 6.0 to less than 2.0 kohm

THIS PAGE INTENTIONALLY LEFT BLANK

APPENDIX B. PROBE ASSEMBLY—LUNA INNOVATIONS NANOFLUID RESISTANCE MEASUREMENTS

*All Resistances in kilo-ohm, Resistance recorded over 10 second immersion

Sample	Solution	A - B	B - C	A - C
402	Initial Conductivity	9.4 - 12.5	7.8 - 11.4	86 - 101
	1st Thaw	68 - 103	14.1 - 19.1	72 - 110
	2nd Thaw	35 - 91	14.1 - 21	105 - 145
	3rd Thaw	50 - 101	142 - 158	221 - 223
	4th Thaw	61 - 111	72 - 103	210 - 219
	5th Thaw	63 - 119	17 - 156	278 - 300
405	Initial Conductivity	41 - 75	6.5 - 13.4	191 - 210
	1st Thaw	48 - 78	12.1 - 16.8	188 - 220
	2nd Thaw	6.2 - 16.5	12.5 - 17.1	258 - 267
	3rd Thaw	45 - 102	30 - 96	229 - 238
	4th Thaw	49 - 113	33 - 102	238 - 246
	5th Thaw	36 - 90	52 - 105	248 - 259
403	Initial Conductivity	11.2 - 15.7	8.6 - 13.2	183 - 200
	1st Thaw	58 - 91	14.6 - 19.1	72 - 110
	2nd Thaw	48 - 112	20 - 80	183 - 220
	3rd Thaw	29 - 65	79 - 114	223 - 226
	4th Thaw	51 - 116	26 - 100	229 - 238
	5th Thaw	27 - 80	80 - 120	262 - 273
406	Initial Conductivity	42 - 79	6.7 - 16.4	96 - 122
	1st Thaw	29 - 79	9.6 - 18	186 - 216
	2nd Thaw	44 - 80	73 - 109	237 - 242
	3rd Thaw	51 - 112	23 - 98	248 - 256
	4th Thaw	44 - 119	23 - 100	256 - 265
	5th Thaw	56 - 108	37 - 95	252 - 262
404	Initial Conductivity	34 - 75	7.6 - 14.2	188 - 199
	1st Thaw	9.4 - 16.2	11.1 - 16.9	91 - 93
	2nd Thaw	33 - 45	91 - 100	48 - 56
	3rd Thaw	35 - 83	50 - 95	217 - 232
	4th Thaw	43 - 105	25 - 92	233 - 240
	5th Thaw	47 - 92	56 - 115	256 - 265
407	Initial Conductivity	45 - 91	8.9 - 12.8	35 - 79
	1st Thaw	8.5 - 17.9	18.1 - 32	101 - 120
	2nd Thaw	46 - 95	56 - 102	244 - 157
	3rd Thaw	50 - 116	24 - 101	253 - 265
	4th Thaw	58 - 124	24 - 90	256 - 263
	5th Thaw	47 - 115	28 - 103	256 - 267

THIS PAGE INTENTIONALLY LEFT BLANK

APPENDIX C. PROBE ASSEMBLY—HOLLOW MULTI-WALL CARBON NANOTUBE RESISTANCE MEASUREMENTS

*All Resistances in kilo-ohm

Sample	Solution	A - B	B - C	A - C	General Notes	
5	Distilled Water	99 - 160	83 - 140	267 - 305	Ultrasonication Power	39 Watts
	Distilled Water / Surf	84 - 119	94 - 106	193 - 228	Time Elapsed until Boiling	(Min:sec)
	Inbetween Stir and Ultra	70 - 100	69 - 102	197 - 225	Sample 5	5:02
	Distilled Water / Surf / CNT	0.75 - 1.1	0.9 - 1.32	3.8 - 4.9	Sample 6	4:59
	1st Thaw	-	-	-	Sample 7	5:31
	2nd Thaw				Sample 8	5:46
6	Distilled Water	140 - 180	92 - 150	298 - 326	Freeze Time (Hours)	6+
	Distilled Water / Surf	52 - 99	24 - 66	190 - 223	1st Thaw Temp	24 °C
	Inbetween Stir and Ultra	-	-	-		
	Distilled Water / Surf / CNT	0.81 - 0.92	0.86 - 1.53	2.6 - 3.5		
	1st Thaw	-	-	-		
	2nd Thaw					
7	Distilled Water	254 - 284	86 - 146	296 - 335		
	Distilled Water / Surf	51 - 92	41 - 97	198 - 245		
	Inbetween Stir and Ultra	76 - 107	25 - 81	190 - 234	- Conductivity Test inbetween Mech Stir and Ultrasonication Test not conducted due to human error	
	Distilled Water / Surf / CNT	0.56 - 0.62	0.78 - 0.84	0.98 - 1.26		
	1st Thaw	-	-	-		
8	Distilled Water	223 - 283	84 - 142	302 - 343	- Heavy agglomeration in all samples after first thaw. Testing Discontinued.	
	Distilled Water / Surf	41 - 98	95 - 120	197 - 232		
	Inbetween Stir and Ultra	49 - 96	22 - 79	183 - 228		
	Distilled Water / Surf / CNT	0.90 - 0.97	1.2 - 1.46	2.56 - 7.1		
	1st Thaw	-	-	-		

Measurement Explanation

- All Resistances in kΩ
- 10 sec Elapsed for Recorded Readings
  - First Number - Initial Reading when leads were clamped
  - Second Number - Reading when 10 seconds elapsed
  - All readings increased - Capacitive effects
- Mechanical Stirring for 30 min prior to Ultrasonication
- Ultrasonication only conducted for solutions with CNT's

Loading	Weight %	Dimension
Surfactant	3.0	0.618 mL
CNT Type	0.5	0.1005 g
Volume of Dist Water	-	20 mL

THIS PAGE INTENTIONALLY LEFT BLANK

APPENDIX D. PROBE ASSEMBLY—BAMBOO MULTI-WALL CARBON NANOTUBE RESISTANCE MEASUREMENTS

Sample	Solution	A - B	B - C	A - C	General Notes	
1	Distilled Water	78 - 160	77 - 128	138 - 175	Ultrasonication Power	39 Watts
	Distilled Water / Surf	71 - 122	68 - 97	75 - 128	Time Elapsed until Boiling (Min:sec)	5:03
	Distilled Water / Surf / CNT	5.5 - 6.2	4.9 - 5.7	5.9 - 7.3	Freeze Temp	-14°C
	First Thaw	-	-	-	Freeze Time (Hours)	6
3	Distilled Water	105 - 181	78 - 170	296 - 334	1st Thaw Temp	23°C
	Distilled Water / Surf	69 - 120	91-112	103 - 136	- Heavy Agglomeration noticed at end of 1st Thaw, conductivity tests not conducted. - CNT precipitated out of solution	
	Distilled Water / Surf / CNT	6.7 - 12.7	8.4 - 12.2	8.9 - 11.8		
	First Thaw	-	-	-		

Sample	Solution	A - B	B - C	A - C	General Notes	
2	Distilled Water	123 - 187	109 - 169	297 - 341	Ultrasonication Power	15 Watts
	Distilled Water / Surf	81 - 121	49 - 99	102 - 133	Time Elapsed until Boiling (Min:sec)	No Boil
	Distilled Water / Surf / CNT	31 - 41	32 - 40	37 - 39	Freeze Temp	-14°C
	First Thaw	-	-	-	Freeze Time (Hours)	6
4	Distilled Water	145 - 199	82 - 176	272 - 350	1st Thaw Temp	23°C
	Distilled Water / Surf	38 - 92	93 - 108	103 - 124	- Heavy Agglomeration noticed at end of 1st Thaw, conductivity tests not conducted. - CNT precipitated out of solution	
	Distilled Water / Surf / CNT	21 - 35	39 - 47	29 - 48		
	First Thaw	-	-	-		

Measurement Explanation

- All Resistances in kΩ
- 10 sec Elapsed for Recorded Readings
  - First Number - Initial Reading when leads were clamped
  - Second Number - Reading when 10 seconds elapsed
  - All readings increased - Capacitive effects
- Mechanical Stirring for 30 min prior to Ultrasonication
- Ultrasonication only conducted for solutions with CNT's

Loading	Weight %	Dimension
Surfactant	3.0	0.618 mL
CNT Type	0.5	0.1005 g
Volume of Dist Water	-	20 mL

THIS PAGE INTENTIONALLY LEFT BLANK

APPENDIX E. LUNA INNOVATION NANOFLUID SURFACE AND BOTTOM RESISTANCE MEASUREMENTS

Surface Resistance (kΩ)						
Insertion	LnW-402	LnW-403	LnW-404	LnW-405	LnW-406	LnW-407
1	11.6	11.7	9.9	5.2	6.9	8.1
2	10.8	11.4	10.1	5.7	7.3	10.1
3	10.8	11.2	12.2	5.8	9.3	9.7
4	11.2	10.0	9.6	5.9	6.9	10.2
5	11.7	10.2	10.3	6.3	7.1	9.6
6	10.2	10.8	9.8	5.5	9.2	8.8
7	10.1	11.3	12.1	6.0	7.4	11.5
8	11.4	10.7	9.9	5.7	12.2	8.7
9	13.2	11.4	10.5	5.8	7.0	9.6
10	10.3	12.8	10.1	5.3	8.2	8.3
11	10.4	10.5	10.3	5.1	11.3	9.0
12	11.3	11.1	9.9	6.3	8.6	10.0
13	10.5	11.3	9.8	6.8	10.6	8.7
14	12.8	11.0	9.9	6.1	7.1	7.9
15	10.9	11.1	10.5	5.9	7.7	8.4
Mean	11.15	11.10	10.33	5.83	8.45	9.24
Std Dev	0.91	0.66	0.79	0.45	1.73	0.98

Bottom Resistance(kΩ)						
Insertion	LnW-402	LnW-403	LnW-404	LnW-405	LnW-406	LnW-407
1	8.3	7.5	6.1	4.4	5.5	6.2
2	8.1	7.5	6.6	4.2	5.3	5.9
3	7.8	8.1	6.0	3.8	4.8	6.4
4	8.2	7.0	6.4	3.9	4.9	6.0
5	7.9	7.3	6.6	3.9	5.0	5.7
6	8.0	6.7	6.5	4.1	4.9	5.9
7	7.4	6.8	6.2	3.8	4.5	6.1
8	8.0	7.1	6.3	3.9	4.7	5.0
9	8.2	7.3	5.9	4.0	5.1	6.1
10	7.9	7.0	6.4	3.7	4.6	5.5
11	8.2	7.3	6.2	3.6	4.7	5.8
12	7.4	7.1	6.1	3.9	5.0	5.6
13	7.6	6.4	6.2	3.6	4.6	5.7
14	7.5	6.6	6.0	4.1	5.1	5.1
15	7.7	7.0	6.4	3.7	4.8	6.0
Mean	7.88	7.11	6.26	3.91	4.90	5.80
Std Dev	0.30	0.42	0.22	0.23	0.28	0.39

THIS PAGE INTENTIONALLY LEFT BLANK

APPENDIX F. MULTIMETER LEAD ORIENTATION RESISTANCE MEASUREMENTS

* All Resistances in kilo-ohm

Sample	Trial	0°	90°	180°	270°
402	1	7.8	7.9	7.8	7.6
	2	7.6	7.8	7.8	7.5
	3	7.7	7.4	7.4	7.5
405	1	4.7	4.7	4.6	4.5
	2	4.0	3.7	3.8	3.8
	3	3.8	3.6	3.8	3.9

THIS PAGE INTENTIONALLY LEFT BLANK

APPENDIX G. NAVAL POSTGRADUATE SCHOOL NANOFLUID RESISTANCE MEASUREMENTS

MWCNT - LDS vs. Igepal Initial Testing
(ICE BATH DURING U/S)

0.2% CNT 3.0% Surf	Sample #1 - LDS								Sample #2 - Igepal							
	DW (MΩ)	DW / LDS	Initial	1st Thaw	2nd Thaw	3rd Thaw	4th Thaw	5th Thaw	DW (MΩ)	DW/ Ige	Initial	1st Thaw	2nd Thaw	3rd Thaw	4th Thaw	5th Thaw
1	0.33	12.3	14.1	8.1	9.7	6.7	7.2	8.4	0.29	32.8	32.8	25.9	27.1	34.4	28.4	26.7
2	0.36	12.1	16.7	9.5	8.8	6.2	6.4	6.7	0.14	34.3	38.6	27.9	34.6	30.0	34.4	25.6
3	0.37	12.4	14.8	9.6	9.0	6.1	6.1	9.1	0.22	38.9	39.6	27.1	31.0	24.5	23.8	34.5
4	0.36	13.4	11.5	10.1	8.0	6.7	5.9	4.8	0.11	38.2	36.0	29.2	42.1	25.3	28.8	21.4
5	0.42	13.6	12.8	9.1	8.6	5.9	5.4	5.5	0.20	41.9	39.5	35.6	35.7	34.0	34.7	23.4
6	0.33	14.4	10.1	8.0	8.7	8.8	7.1	6.3	0.18	42.5	40.0	36.7	30.4	28.0	28.5	24.1
7	0.30	14.7	11.6	7.4	9.2	7.8	6.6	6.7	0.21	36.3	34.6	31.7	28.6	33.7	28.0	25.3
8	0.34	14.0	11.4	7.0	7.9	6.5	7.1	7.3	0.22	32.4	42.2	34.5	29.7	31.2	31.5	22.6
9	0.32	13.5	12.6	7.2	8.0	7.4	7.3	7.8	0.25	39.6	35.0	31.5	29.1	28.5	31.3	23.1
10	0.32	12.1	10.6	8.0	7.1	7.2	5.7	3.9	0.12	39.8	36.9	26.2	32.5	24.6	30.9	30.8
11	0.34	12.4	10.4	9.1	7.5	7.9	5.1	6.6	0.17	44.1	36.6	27.5	30.3	25.3	35.5	23.1
12	0.39	14.3	10.0	6.6	8.0	6.0	8.5	7.0	0.21	40.5	42.3	31.9	33.1	34.1	33.4	28.0
13	0.31	13.7	12.9	7.0	8.1	6.9	7.4	9.3	0.13	40.6	39.4	32.5	27.1	28.4	32.9	32.0
14	0.33	14.1	12.3	11.1	8.6	7.4	8.7	8.3	0.16	44.1	34.7	26.5	28.4	37.0	29.2	25.4
15	0.33	15.1	11.8	10.1	9.3	7.1	6.5	9.3	0.18	38.3	37.5	30.7	29.1	34.9	33.2	30.5
Mean	0.34	13.47	12.24	8.53	8.43	6.97	6.73	7.13	0.19	38.95	37.71	30.36	31.25	30.26	30.97	26.43
Std Dev	0.03	1.00	1.86	1.38	0.71	0.81	1.04	1.62	0.05	3.69	2.83	3.52	3.93	4.24	3.18	3.91

Notes
- Hollow MWCNT, 20 mL Sample
- All Resistances in k-Ohm
- Ultrasonicated at 15W for 15 Min, Sample at 21°C
- 0.2% vol CNT (0.04 g)
- 3.0% Surfactant (0.6 g)

1st Thaw - Light Sediment at bottom
2nd Thaw - Small Agglomerates and Sediment at Bottom
3rd Thaw - Small Agglomerates and Sediment at Bottom
4th Thaw - Small Agglomerates and Sediment at Bottom
5th Thaw - Small Agglomerates and Sediment at Bottom

1st Thaw - Light Sediment at bottom
2nd Thaw - Small Agglomerates and Sediment at Bottom
3rd Thaw - Small Agglomerates and Sediment at Bottom
4th Thaw - Medium Agglomerates and Sediment
5th Thaw - Medium and Large Agglomerates and Sediment

SWCNT - LDS vs. Igepal Initial Testing
(ICE BATH DURING U/S)

0.2% CNT 3.0% Surf	Sample #3 - LDS								Sample #4 - Igepal							
	DW (MΩ)	DW / LDS	Initial	1st Thaw	2nd Thaw	3rd Thaw	4th Thaw	5th Thaw	DW (MΩ)	DW/ Ige	Initial	1st Thaw	2nd Thaw	3rd Thaw	4th Thaw	5th Thaw
1	0.23	9.3	6.3	10.4	10.5	6.9	6.9	5.7	0.21	29.9	31.8	25.2	27.1	29.9		
2	0.32	12.0	6.5	6.4	11.5	8.5	6.7	5.3	0.22	33.0	35.5	29.1	27.2	29.6		
3	0.22	12.5	7.1	7.1	7.2	7.8	5.6	4.5	0.26	37.6	32.0	29.7	29.9	28.7		
4	0.28	14.6	6.0	7.7	10.2	6.5	8.6	5.2	0.24	36.5	41.3	30.8	33.2	32.2		
5	0.21	15.1	6.4	9.4	9.3	6.0	7.8	5.9	0.23	38.5	36.6	31.0	31.6	22.1		
6	0.22	14.0	5.3	7.2	10.6	7.4	8.2	7.2	0.30	39.6	30.7	29.4	29.2	23.7		
7	0.25	15.3	5.5	8.5	9.9	8.3	8.7	8.0	0.28	37.0	42.4	29.5	30.6	25.8		
8	0.24	12.6	5.7	9.1	10.1	8.1	8.1	8.5	0.21	31.2	41.7	30.3	35.0	27.9	Sample Unstable	
9	0.19	14.5	6.3	10.5	10.2	10.0	7.9	9.3	0.19	33.1	35.0	32.5	29.2	30.1		
10	0.28	15.8	5.8	11.1	9.4	8.5	8.7	7.6	0.31	34.7	43.1	31.7	31.8	30.4	Testing Discontinued	
11	0.23	12.2	5.7	7.5	11.0	7.1	8.9	9.0	0.24	34.0	37.8	33.7	29.6	29.4		
12	0.22	14.7	6.0	8.5	11.2	11.5	9.6	8.0	0.22	35.5	42.5	33.0	30.0	28.0		
13	0.20	14.1	6.3	9.6	10.6	10.6	9.8	7.8	0.23	34.8	35.0	30.2	30.3	32.7		
14	0.18	13.0	5.2	9.9	10.4	9.1	9.3	8.6	0.22	35.1	29.9	30.8	27.4	30.6		
15	0.25	14.6	6.1	7.5	11.0	7.6	9.0	8.3	0.19	32.3	31.2	31.6	31.0	33.4		
Mean	0.23	13.62	6.01	8.69	10.21	8.26	8.25	7.26	0.24	34.86	36.43	30.57	30.21	28.97		
Std Dev	0.04	1.69	0.50	1.44	1.03	1.53	1.15	1.54	0.04	2.71	4.78	2.01	2.18	3.15		

Notes
- SWCNT, 20 mL Sample
- All Resistances in k-Ohm
- Ultrasonicated at 15W for 15 Min, , Sample at 21°C
- 0.2% vol CNT (0.04 g)
- 3.0% Surfactant (0.6 g)

1st Thaw - Light Sediment at bottom
2nd Thaw - Light Sediment at bottom
3rd Thaw - Small Agglomerates and Sediment at Bottom
4th Thaw - Small Agglomerates and Sediment at Bottom
5th Thaw - Small Agglomerates and Sediment at Bottom

1st Thaw - Light Sediment at bottom
2nd Thaw - Light sediment at Bottom
3rd Thaw - Sample Unstable - Layered Appearance - Heavy Sediment at Bottom

MWCNT - LDS vs. Igepal Initial Testing
(ICE BATH DURING U/S)

0.1% CNT 3.0% Surf	Sample #5 - LDS								Sample #6 - Igepal							
	DW (MΩ)	DW / LDS	Initial	1st Thaw	2nd Thaw	3rd Thaw	4th Thaw	5th Thaw	DW (MΩ)	DW/ Ige	Initial	1st Thaw	2nd Thaw	3rd Thaw	4th Thaw	5th Thaw
1	0.26	9.7	8.9	8.0	11.1	10.7	9.2	5.7	0.21	28.2	34.1	27.8	24.2	36.0	23.8	22.0
2	0.33	12.7	7.9	6.3	8.3	11.1	9.7	6.3	0.29	28.8	32.7	28.9	26.6	31.5	24.0	26.3
3	0.21	12.9	8.8	6.5	7.8	12.1	7.2	7.5	0.33	29.5	35.7	35.4	32.5	28.0	27.2	23.5
4	0.31	14.2	10.0	7.1	10.3	10.6	7.4	4.0	0.28	36.5	35.6	25.4	29.1	28.8	23.6	25.2
5	0.40	15.8	10.1	7.9	8.6	9.1	10.2	6.4	0.21	32.1	39.5	28.6	29.6	39.9	24.7	23.9
6	0.36	17.3	9.2	9.1	11.1	10.8	8.6	7.0	0.19	35.7	37.1	40.1	27.1	30.9	27.3	35.2
7	0.37	14.2	9.1	8.0	9.3	9.8	8.0	7.8	0.20	35.8	40.4	28.1	27.9	29.2	30.9	20.4
8	0.25	15.9	10.8	7.7	9.9	10.5	8.6	6.7	0.27	37.0	37.0	27.3	31.3	29.8	28.9	20.6
9	0.26	16.6	9.6	8.1	10.0	8.6	7.8	8.1	0.23	34.3	40.1	29.9	23.4	27.1	30.9	22.0
10	0.25	16.4	9.8	9.2	11.0	10.8	8.8	6.6	0.20	36.4	37.5	28.0	22.6	32.2	29.7	24.1
11	0.22	14.0	7.8	8.6	10.3	11.5	9.1	9.0	0.22	34.6	32.7	30.6	26.5	23.8	24.7	21.8
12	0.20	17.0	11.3	7.5	10.8	8.8	9.0	8.0	0.28	41.2	34.7	28.5	25.0	33.4	27.8	26.1
13	0.28	15.9	10.4	10.5	10.2	8.9	9.4	8.6	0.21	39.0	36.6	27.8	28.0	29.8	31.8	25.0
14	0.29	15.5	9.8	7.9	8.5	9.5	9.1	7.0	0.19	40.5	39.1	34.7	34.0	29.6	31.3	29.9
15	0.25	16.3	11.3	8.7	10.6	9.9	8.2	8.9	0.22	38.8	35.2	31.6	32.6	28.1	33.2	24.4
Mean	0.28	14.96	9.65	8.07	9.85	10.18	8.69	7.17	0.24	35.23	36.53	30.18	28.03	30.54	24.70	24.69
Std Dev	0.06	2.04	1.07	1.07	1.09	1.05	0.84	1.33	0.04	4.07	2.49	3.84	3.49	3.83	3.26	3.81

Notes
- Hollow MWCNT, 20 mL Sample
- All Resistances in k-Ohm
- Ultrasonicated at 15W for 15 Min, , Sample at 21°C
- 0.1% vol CNT (0.02 g)
- 3.0% Surfactant (0.6 g)

1st Thaw - Small Agglomerates at bottom
2nd Thaw - Small Agglomerates at bottom
3rd Thaw - Small Agglomerates at bottom
4th Thaw - Medium and Small Agglomerates and Suspensions
5th Thaw - Large Agglomerates and Suspensions at Bottom

1st Thaw - Light Sediment at Bottom
2nd Thaw - Very small agglomerates at Bottom
3rd Thaw - Very small agglomerates at Bottom
4th Thaw - Very small agglomerates at Bottom
5th Thaw - Very small agglomerates at Bottom

SWCNT - LDS vs. Igepal Initial Testing
(ICE BATH DURING U/S)

0.1% CNT 3.0% Surf	Sample #7 - LDS								Sample #8 - Igepal							
	DW (MΩ)	DW / LDS	Initial	1st Thaw	2nd Thaw	3rd Thaw	4th Thaw	5th Thaw	DW (MΩ)	DW/ Ige	Initial	1st Thaw	2nd Thaw	3rd Thaw	4th Thaw	5th Thaw
1	0.21	9.2	5.5	12.9	12.2	9.5	7.1	7.1	0.25	28.2	43.0	27.4	30.4	25.5		
2	0.19	11.3	5.2	12.0	12.9	9.3	9.6	7.7	0.26	32.2	45.9	30.2	26.7	25.3		
3	0.25	12.0	6.0	14.5	9.7	9.4	7.9	7.1	0.30	31.3	44.2	29.5	28.7	29.9		
4	0.18	12.4	6.3	13.6	11.3	9.8	9.2	7.5	0.29	37.0	39.2	27.8	26.5	22.6		
5	0.19	12.2	5.8	12.3	12.1	9.7	10.2	7.7	0.32	33.0	45.7	29.2	24.7	25.0		
6	0.26	11.4	5.4	13.1	11.1	10.6	8.8	9.3	0.25	38.5	41.8	32.2	29.3	26.4		
7	0.27	14.8	5.7	9.7	12.4	11.2	6.1	9.0	0.24	33.4	35.2	34.8	27.4	23.8		
8	0.19	13.9	4.9	12.9	13.0	11.1	8.3	9.1	0.28	33.9	37.0	33.8	29.1	25.9	Sample Unstable	
9	0.20	13.6	5.4	9.6	11.9	11.3	9.7	8.5	0.29	31.9	41.7	29.2	26.8	26.8		
10	0.22	17.1	5.7	10.6	11.8	10.8	11.3	9.6	0.25	32.8	33.5	27.6	29.5	22.1	Testing Discontinued	
11	0.19	14.0	4.9	12.1	12.0	10.7	9.7	10.8	0.26	37.1	40.4	32.7	32.1	22.6		
12	0.20	16.6	6.4	13.8	11.5	9.1	10.5	9.9	0.24	39.1	36.2	30.3	28.9	28.9		
13	0.19	16.7	6.2	13.1	11.3	11.1	9.6	11.0	0.18	41.6	47.1	31.3	33.6	26.2		
14	0.29	14.4	5.1	11.2	14.2	10.4	11.6	7.2	0.28	35.3	39.5	33.9	32.4	28.9		
15	0.24	13.5	5.2	10.9	12.9	11.3	8.2	9.4	0.27	33.5	38.0	36.1	30.5	26.5		
Mean	0.22	13.54	5.58	12.15	12.02	10.35	9.19	8.73	0.26	34.59	40.56	31.07	29.11	25.76		
Std Dev	0.04	2.21	0.49	1.48	1.04	0.80	1.50	1.31	0.03	3.49	4.14	2.75	2.45	2.35		

Notes
- SWCNT, 20 mL Sample
- All Resistances in k-Ohm
- Ultrasonicated at 15W for 15 Min, , Sample at 21°C
- 0.1% vol CNT (0.02 g)
- 3.0% Surfactant (0.6 g)

1st Thaw - Light Sediment at Bottom
2nd Thaw - Light Sediment at Bottom
3rd Thaw - Light Sediment at Bottom
4th Thaw - Light Sediment at Bottom
5th Thaw - Light Sediment at Bottom

1st Thaw - Light Sediment at Bottom
2nd Thaw - Heavier Sediment Layer at Bottm
3rd Thaw - Sample Unstable - Layered Apperance
- Heavy Sediment at Bottom

MWCNT - LDS vs. Igepal Initial Testing																
0.2% CNT 3.0% Surf	Sample #9 - LDS								Sample #10 - Igepal							
	DW (MΩ)	DW / LDS	Initial	1st Thaw	2nd Thaw	3rd Thaw	4th Thaw	5th Thaw	DW (MΩ)	DW/ Ige	Initial	1st Thaw	2nd Thaw	3rd Thaw	4th Thaw	5th Thaw
1	0.61	10.9	3.2	10.1	7.3	6.0	7.9	4.8	0.71	38.8	17.2	24.8	24.4	24.0	23.5	34.9
2	0.62	8.2	1.7	9.7	5.6	2.5	6.6	4.6	0.65	36.4	17.9	29.6	29.8	22.4	21.8	24.5
3	0.70	7.9	2.8	8.3	7.7	1.9	6.8	2.9	0.69	40.0	16.0	28.5	32.2	26.0	28.2	31.2
4	0.69	9.1	1.5	7.7	5.7	3.1	9.2	4.4	0.80	34.5	14.0	24.4	33.6	23.7	26.8	26.4
5	0.72	8.6	1.4	7.3	4.5	0.6	8.6	5.1	0.65	35.0	15.7	31.4	31.1	21.5	25.2	27.1
6	0.73	9.3	3.0	9.2	6.4	5.8	9.1	4.5	0.72	36.0	12.3	33.2	33.9	23.6	27.2	26.5
7	0.65	9.2	3.1	8.0	7.1	6.1	6.4	6.2	0.60	37.0	17.0	32.0	29.3	21.4	22.6	29.4
8	0.71	9.4	2.0	7.6	8.5	6.7	7.4	6.1	0.65	35.9	12.3	31.8	28.1	28.9	29.8	26.5
9	0.67	10.8	2.5	7.8	7.7	7.1	8.7	5.2	0.66	36.3	15.5	26.6	26.3	26.0	31.6	27.7
10	0.70	9.9	3.4	7.7	7.8	8.7	9.8	6.7	0.71	37.6	15.8	25.6	34.4	26.4	31.9	26.3
11	0.93	11.5	2.2	7.8	8.9	8.9	8.2	4.8	0.75	38.7	17.1	30.7	31.2	23.2	32.9	24.2
12	0.73	12.5	2.7	7.4	8.7	8.0	9.1	5.6	0.70	40.1	13.2	31.9	27.5	28.6	27.5	28.2
13	0.80	10.3	2.6	9.5	9.0	7.2	8.4	6.0	0.62	42.4	17.0	27.9	38.1	24.5	26.2	28.9
14	0.63	11.3	3.0	7.6	9.4	6.1	10.0	5.4	0.64	35.4	15.5	35.2	24.9	27.9	27.9	24.1
15	0.71	9.2	3.1	7.8	8.6	7.8	9.2	5.2	0.65	35.2	17.2	30.6	28.8	25.6	27.6	27.4
Mean	0.71	9.87	2.55	8.23	7.53	5.77	8.36	5.17	0.68	37.29	15.58	29.61	30.24	24.91	27.38	27.55
Std Dev	0.08	1.31	0.64	0.92	1.44	2.56	1.13	0.93	0.05	2.27	1.83	3.22	3.80	2.40	3.29	2.81

Notes

- Hollow MWCNT, 20 mL Sample
- All Resistances in k-Ohm, except DW for 15 Min
- 0.2% vol CNT (0.04 g)
- 3.0% Surfactant (0.6 g)

Max Temp during U/S - 73°C, Sample Stable
1st Thaw - Small Agglomerates at Bottom
2nd Thaw - Small Agglomerates at Bottom
3rd Thaw - Medium Agglomerates and Sediment
4th Thaw - Medium Agglomerates and Sediment
5th Thaw - Medium Agglomerates and Sediment

Max Temp during U/S- 73°C, Sample Stable
1st Thaw - Small Agglomerates at Bottom
2nd Thaw - Small Agglomerates and Sediment
3rd Thaw - Large Agglomerates and Sediment
4th Thaw - Large Agglomerates and Sediment
5th Thaw - Large Agglomerates and Sediment

- Ultrasonicated at 15W

SWCNT - LDS vs. Igepal Initial Testing																
0.2% CNT 3.0% Surf	Sample #11 - LDS								Sample #12 - Igepal							
	DW (MΩ)	DW / LDS	Initial	1st Thaw	2nd Thaw	3rd Thaw	4th Thaw	5th Thaw	DW (MΩ)	DW/ Ige	Initial	1st Thaw	2nd Thaw	3rd Thaw	4th Thaw	5th Thaw
1	0.75	10.2	3.6	8.5	6.0	6.8	6.5	4.4	0.52	33.1						
2	0.80	11.1	3.5	8.8	6.5	5.1	4.3	9.8	0.55	34.8						
3	0.79	9.8	3.3	7.9	8.1	6.6	7.5	7.0	0.48	29.7						
4	0.67	12.3	3.7	6.4	8.2	7.2	7.4	8.6	0.52	29.1						
5	0.71	13.6	3.2	8.7	7.9	8.0	8.9	9.0	0.49	28.8						
6	0.64	11.5	3.3	7.8	8.3	8.9	10.5	8.5	0.48	30.3						
7	0.82	10.3	3.4	9.4	8.8	6.6	7.4	9.8	0.51	33.0						
8	0.75	12.5	3.6	10.0	8.3	7.5	7.2	7.2	0.53	32.4	Sample Unstable after U/S					
9	0.71	14.2	3.9	9.6	8.7	9.6	8.8	9.4	0.57	34.3						
10	0.66	13.6	3.3	10.4	8.3	12.3	8.5	9.8	0.49	33.1	Testing Discontinued					
11	0.62	13.6	3.4	8.7	8.5	8.6	10.2	5.2	0.60	34.5						
12	0.65	13.0	3.7	9.1	9.3	9.5	11.0	9.6	0.49	29.9						
13	0.68	14.0	3.9	9.5	7.2	7.1	8.1	9.0	0.48	31.0						
14	0.71	9.7	3.3	10.0	8.2	9.5	7.5	9.2	0.52	28.7						
15	0.63	10.7	3.1	9.9	8.7	9.3	9.0	9.6	0.50	28.4						
Mean	0.71	12.01	3.48	8.98	8.07	8.17	8.19	8.41	0.52	31.41						
Std Dev	0.06	1.62	0.25	1.05	0.88	1.76	1.69	1.71	0.04	2.30						

Notes

- SWCNT, 20 mL Sample
- All Resistances in k-Ohm, excpet DW
- Ultrasonicated at 15W for 15 Min
- 0.2% vol CNT (0.04 g)
- 3.0% Surfactant (0.6 g)

Max Temp during U/S - 70°C, Sample Stable
1st Thaw - Light Sediment at bottom
2nd Thaw - Light Sediment at bottom
3rd Thaw - Light Sediment at bottom
4th Thaw - Light Sediment at bottom
5th Thaw - Light Sediment at bottom

Max Temp during U/S- 74°C, Sample Unstable
- Layered Separation after U/S -> Heavy sediment at bottom with small agglomerates

MWCNT - LDS vs. Igepal Initial Testing																
0.1% CNT 3.0% Surf	Sample #13 - LDS								Sample #14 - Igepal							
	DW (MΩ)	DW / LDS	Initial	1st Thaw	2nd Thaw	3rd Thaw	4th Thaw	5th Thaw	DW (MΩ)	DW/ Ige	Initial	1st Thaw	2nd Thaw	3rd Thaw	4th Thaw	5th Thaw
1	0.63	9.9	4.2	10.6	6.6	6.4	5.0	7.7	0.65	32.2	10.5	30.0	23.3	20.3	25.9	28.8
2	0.66	7.1	5.1	10.2	6.8	5.5	6.5	9.1	0.67	28.4	9.8	27.7	18.8	25.6	33.3	27.5
3	0.71	9.8	4.8	7.3	8.0	7.1	5.8	9.8	0.61	28.5	10.6	32.6	24.7	21.1	29.5	37.5
4	0.56	8.4	5.3	7.8	7.5	12.1	6.6	7.9	0.60	33.4	11.1	31.2	26.6	24.9	34.9	32.5
5	0.55	8.9	3.7	9.5	8.8	8.6	8.3	9.5	0.59	31.7	14.3	29.7	23.1	26.2	28.2	29.3
6	0.59	9.2	5.5	8.0	9.5	6.2	7.2	10.4	0.71	33.8	12.3	27.6	24.6	31.3	34.5	27.1
7	0.68	9.4	4.8	7.1	6.1	6.1	8.6	8.9	0.69	32.1	12.7	28.8	26.9	27.4	26.4	36.2
8	0.62	8.6	3.6	8.9	7.1	8.0	10.3	8.8	0.68	29.3	12.3	29.6	25.6	19.4	32.0	35.3
9	0.57	9.3	4.0	8.0	9.2	7.4	9.3	12.4	0.62	36.8	12.1	33.3	27.6	22.7	34.4	32.4
10	0.54	10.0	4.7	7.7	8.9	6.8	9.1	11.0	0.65	34.7	10.9	27.8	29.1	30.7	31.7	28.0
11	0.61	9.9	4.8	7.6	9.5	5.4	7.2	9.0	0.63	35.7	11.9	27.0	25.0	29.4	28.6	29.1
12	0.70	8.4	6.0	8.5	8.5	7.5	7.1	10.4	0.70	36.8	13.6	28.4	27.2	27.3	33.0	31.5
13	0.68	7.8	5.1	8.1	8.7	8.8	10.5	12.4	0.69	32.4	12.9	27.6	29.3	23.8	31.9	27.8
14	0.55	8.8	4.8	7.9	8.3	5.6	8.1	11.8	0.59	30.1	12.1	30.8	23.2	24.0	25.8	32.1
15	0.59	9.0	2.9	8.2	9.1	6.2	8.7	10.8	0.63	32.3	13.3	32.5	28.3	31.8	31.7	33.8
Mean	0.62	8.97	4.62	8.36	8.17	7.18	7.89	9.99	0.65	32.55	12.03	29.64	25.55	25.73	30.79	31.26
Std Dev	0.06	0.82	0.81	1.02	1.10	1.73	1.59	1.49	0.04	2.73	1.26	2.05	2.78	3.96	3.17	3.36

Notes
- Hollow MWCNT, 20 mL Sample
- All Resistances in k-Ohm, except DW
- Ultrasonicated at 15W for 15 Min
- 0.1% vol CNT (0.02 g)
- 3.0% Surfactant (0.6 g)

Max Temp during U/S - 72°C, Sample Stable
1st Thaw - Small Agglomerates at Bottom
2nd Thaw - Small Agglomerates at Bottom
3rd Thaw - Small Agglomerates at Bottom
4th Thaw - Small Agglomerates at Bottom
5th Thaw - Small Agglomerates at Bottom

Max Temp during U/S- 77°C, Sample Stable
1st Thaw - Very Small Agglomerates at Bottom
2nd Thaw - Small Agglomerates at Bottom
3rd Thaw - Small Agglomerates at Bottom
4th Thaw - Small Agglomerates at Bottom
5th Thaw - Small Agglomerates at Bottom

SWCNT - LDS vs. Igepal Initial Testing																
0.1% CNT 3.0% Surf	Sample #15 - LDS								Sample #16 - Igepal							
	DW (MΩ)	DW / LDS	Initial	1st Thaw	2nd Thaw	3rd Thaw	4th Thaw	5th Thaw	DW (MΩ)	DW/ Ige	Initial	1st Thaw	2nd Thaw	3rd Thaw	4th Thaw	5th Thaw
1	0.53	8.2	5.5	9.3	7.2	6.2	4.5	4.2	0.61	25.4						
2	0.56	9.7	6.2	8.1	6.4	7.9	4.9	5.4	0.65	34.1						
3	0.52	9.6	5.3	8.4	8.7	9.0	5.3	6.4	0.59	27.9						
4	0.57	9.5	5.8	8.5	8.0	8.1	7.1	7.2	0.57	27.8						
5	0.53	7.3	7.1	9.4	9.5	9.4	5.1	8.6	0.62	26.5						
6	0.54	8.2	6.0	9.0	8.6	9.1	7.5	9.6	0.55	30.3						
7	0.55	8.3	4.5	9.6	9.7	8.2	6.0	9.5	0.61	29.9						
8	0.59	8.0	5.1	12.2	10.0	9.3	6.5	7.2	0.60	28.4	Sample Unstable after U/S					
9	0.63	8.2	4.8	10.0	9.0	11.7	8.5	8.6	0.70	27.7						
10	0.51	10.1	5.4	9.8	9.4	11.4	5.9	7.3	0.62	34.4	Testing Discontinued					
11	0.65	9.4	5.3	7.8	9.3	9.6	6.0	9.1	0.64	29.2						
12	0.51	8.8	5.7	9.5	10.9	8.4	7.1	9.6	0.63	30.7						
13	0.52	9.3	5.4	11.2	10.8	10.1	7.5	10.4	0.60	28.9						
14	0.55	9.1	4.9	8.7	8.3	8.9	7.7	10.1	0.62	29.1						
15	0.60	9.0	6.2	10.4	8.7	10.5	9.5	8.0	0.59	32.7						
Mean	0.56	8.85	5.55	9.46	8.97	9.19	6.61	8.08	0.61	29.53						
Std Dev	0.04	0.78	0.65	1.17	1.21	1.40	1.41	1.79	0.04	2.59						

Notes
- SWCNT, 20 mL Sample
- All Resistances in k-Ohmexcept DW
- Ultrasonicated at 15W for 15 Min
- 0.1% vol CNT (0.02 g)
- 3.0% Surfactant (0.6 g)

Max Temp during U/S - 69°C, Sample Stable
1st Thaw - Light Sediment at Bottom
2nd Thaw - Light Sediment at Bottom
3rd Thaw - Light Sediment at Bottom
4th Thaw - Light Sediment at Bottom
5th Thaw - Light Sediment at Bottom

Max Temp during U/S- 72°C, Sample Unstable
- Layered Separation after U/S -> Heavy sediment at bottom with small agglomerates

APPENDIX H. LUNA INNOVATIONS NANOFLUID RESISTANCE MEASUREMENTS

*All Resistances in kilo-ohm

LnW - 402 Resistance (kΩ)										
Insertion	Initial	Thaw #1	Thaw #2	Thaw #3	Thaw #4	Thaw #5	Thaw #6	Thaw #12	Re-Son	Thaw #1
1	11.2	12.3	14.0	12.0	13.5	8.5	10.0	21.6	7.6	10.2
2	10.6	11.4	14.2	12.2	12.3	8.9	9.2	17.4	8.2	13.3
3	10.9	11.7	10.8	11.7	12.6	7.8	10.2	18.4	8.5	11.0
4	10.1	10.8	12.7	13.4	13.5	8.6	9.1	21.0	8.0	11.1
5	10.5	11.8	14.9	12.6	11.7	8.3	9.3	20.9	6.4	12.7
6	11.0	12.7	11.5	11.8	12.3	8.9	9.5	22.0	7.6	9.5
7	10.9	11.7	13.8	11.5	13.4	8.4	9.6	27.9	7.7	11.0
8	10.4	12.2	11.7	11.9	13.0	8.6	10.1	23.1	8.1	10.6
9	10.8	11.6	12.1	12.6	12.9	9.1	10.4	23.7	8.0	10.1
10	11.0	11.9	13.6	12.0	12.3	9.7	10.1	19.5	7.2	11.1
11	10.6	12.7	14.1	11.3	13.0	8.6	10.2	21.9	8.4	11.7
12	12.1	11.3	12.0	13.5	12.7	8.2	9.8	23.4	8.0	12.8
13	10.4	12.1	11.5	11.7	12.6	10.1	12.5	20.8	8.9	13.5
14	9.9	13.1	11.7	12.7	11.9	9.3	9.6	19.5	6.5	15.6
15	10.6	11.4	13.7	10.9	12.8	8.6	10.0	22.1	6.8	13.4
Mean	10.73	11.91	12.82	12.12	12.70	8.77	9.97	21.55	7.73	11.84
Std Dev	0.52	0.61	1.28	0.73	0.54	0.59	0.80	2.51	0.73	1.66

LnW - 403 Resistance (kΩ)										
Insertion	Initial	Thaw #1	Thaw #2	Thaw #3	Thaw #4	Thaw #5	Thaw #6	Thaw #12	Re-Son	Thaw #1
1	9.1	11.7	12.0	11.8	12.3	8.4	9.3	18.4	4.4	12.8
2	8.4	11.3	10.6	10.5	12.0	9.5	9.0	18.1	7.1	10.3
3	8.9	10.7	13.2	10.7	13.3	9.0	10.3	20.5	6.3	10.4
4	8.2	11.7	12.0	11.7	12.4	9.8	9.6	25.1	7.1	11.9
5	8.0	11.4	11.4	11.6	12.8	9.9	9.9	22.8	7.0	10.3
6	8.3	11.5	11.0	9.5	12.7	8.4	9.5	19.6	7.5	10.5
7	9.1	11.2	11.3	11.2	12.9	9.9	9.9	16.7	6.9	11.6
8	8.3	10.5	12.0	11.6	11.9	9.5	9.3	20.5	6.7	12.3
9	8.5	12.2	11.0	12.7	11.5	8.3	9.0	18.8	5.5	10.3
10	8.2	11.6	10.9	12.4	12.2	8.7	10.4	20.8	7.2	12.2
11	8.8	10.9	11.5	11.3	12.9	9.0	10.1	22.6	7.9	11.6
12	8.9	10.8	12.2	11.5	12.3	9.5	10.2	21.8	7.4	13.3
13	8.3	11.6	11.0	12.6	11.6	8.6	10.5	20.6	8.2	9.9
14	8.7	10.9	11.8	10.9	11.9	9.7	10.2	21.7	7.0	10.6
15	9.0	11.5	11.3	11.1	11.8	8.7	9.5	20.1	7.9	10.5
Mean	8.58	11.30	11.55	11.41	12.30	9.13	9.78	20.54	6.94	11.23
Std Dev	0.37	0.46	0.67	0.84	0.53	0.59	0.50	2.11	0.97	1.07

*All Resistances in kilo-ohm

LnW - 404 Resistance (kΩ)										
Insertion	**Initial**	**Thaw #1**	**Thaw #2**	**Thaw #3**	**Thaw #4**	**Thaw #5**	**Thaw #6**	**Thaw #12**	**Re-Son**	**Thaw #1**
1	8.6	8.4	9.6	9.8	8.9	8.9	9.0	15.4	5.1	6.3
2	7.4	9.3	9.4	7.8	9.2	7.7	8.5	15.6	6.4	3.9
3	7.2	8.8	9.5	7.3	9.1	8.4	9.2	16.1	6.7	3.4
4	7.4	8.8	7.9	9.0	7.8	8.7	9.0	19.4	6.5	6.7
5	7.9	9.7	9.1	9.2	7.3	8.3	7.4	17.6	7.5	7.1
6	7.6	9.4	8.4	8.8	7.4	7.8	9.0	18.8	6.8	8.2
7	8.1	9.7	9.3	9.3	7.4	9.8	8.6	15.2	6.9	7.3
8	7.4	8.7	9.0	9.0	8.5	8.6	9.9	17.1	6.6	8.5
9	7.9	9.1	9.5	8.5	8.3	8.3	8.5	18.5	6.4	5.4
10	8.2	9.5	8.4	7.8	7.9	9.2	8.1	16.8	7.5	7.9
11	8.0	9.1	8.0	9.5	8.2	9.7	8.9	23.5	7.1	6.4
12	7.5	9.2	8.8	8.6	8.4	8.6	8.5	17.5	6.4	8.0
13	8.3	8.3	9.3	9.8	7.8	7.6	9.6	21.5	7.2	7.7
14	8.1	8.7	9.2	9.0	8.9	8.0	9.1	16.7	6.3	11.7
15	7.7	9.0	8.4	9.4	9.0	8.3	8.9	18.8	7.2	9.9
Mean	7.82	9.05	8.92	8.85	8.27	8.53	8.81	17.90	6.71	7.23
Std Dev	0.40	0.43	0.57	0.74	0.65	0.66	0.60	2.30	0.60	2.10

LnW - 405 Resistance (kΩ)										
Insertion	**Initial**	**Thaw #1**	**Thaw #2**	**Thaw #3**	**Thaw #4**	**Thaw #5**	**Thaw #6**	**Thaw #12**	**Re-Son**	**Thaw #1**
1	5.1	6.9	7.3	6.4	7.1	4.8	6.4	13.1	5.7	8.7
2	4.9	6.9	7.2	8.2	6.9	5.7	6.9	13.5	6.0	11.5
3	5.3	8.0	7.8	7.0	8.9	4.6	6.7	13.0	6.1	9.1
4	4.6	6.3	8.4	8.2	6.4	4.7	6.9	12.3	6.2	9.5
5	4.6	7.3	7.3	7.0	6.2	5.1	6.5	16.0	6.8	9.3
6	4.2	6.9	7.7	6.7	6.3	5.4	6.8	11.8	6.0	10.3
7	4.5	6.1	7.3	8.1	5.9	4.6	6.0	13.0	6.3	9.2
8	4.4	6.8	6.6	7.2	6.2	5.9	6.2	13.8	6.7	9.1
9	5.0	6.2	6.7	8.2	5.7	4.9	6.1	16.0	7.2	10.9
10	4.7	6.7	7.0	6.9	5.8	4.3	5.8	13.0	6.1	11.5
11	4.6	6.1	7.4	7.4	5.7	5.0	5.7	11.0	6.3	10.5
12	4.9	6.3	8.2	6.8	6.0	6.1	5.9	12.5	6.9	11.1
13	4.8	6.7	6.6	7.2	6.3	4.6	6.2	13.4	7.4	9.7
14	4.2	6.2	7.3	7.0	5.4	5.7	7.0	12.6	7.0	9.9
15	4.6	6.8	6.8	6.9	5.7	5.1	6.2	12.4	6.3	8.4
Mean	4.69	6.68	7.31	7.28	6.30	5.10	6.35	13.16	6.47	9.91
Std Dev	0.31	0.52	0.54	0.60	0.85	0.54	0.43	1.35	0.50	1.00

*All Resistances in kilo-ohm

LnW - 406 Resistance (kΩ)										
Insertion	**Initial**	**Thaw #1**	**Thaw #2**	**Thaw #3**	**Thaw #4**	**Thaw #5**	**Thaw #6**	**Thaw #12**	**Re-Son**	**Thaw #1**
1	6.2	9.1	7.4	7.6	6.3	6.2	7.2	9.4	8.0	7.0
2	6.4	8.6	8.6	8.2	7.4	6.7	7.3	11.0	7.8	8.2
3	6.9	9.2	8.7	9.4	7.7	5.6	7.6	10.1	7.7	8.4
4	6.6	9.5	8.5	8.4	7.1	6.2	7.3	11.2	8.1	8.9
5	6.3	9.9	8.2	7.6	7.6	7.3	7.4	13.2	8.0	9.1
6	6.0	9.2	7.9	9.6	8.6	7.0	6.9	13.7	9.1	9.5
7	6.2	10.6	7.8	8.8	7.3	5.9	7.3	13.3	5.6	11.4
8	6.1	8.9	8.9	9.1	6.2	6.5	7.9	10.1	7.3	9.5
9	6.9	8.6	8.2	8.2	7.7	6.9	7.8	11.4	7.0	10.3
10	6.3	8.9	9.3	9.3	8.1	8.1	7.7	12.1	6.4	8.5
11	6.5	9.7	8.9	8.7	7.2	7.5	7.8	14.9	7.3	10.7
12	6.9	9.8	7.9	9.2	7.8	6.1	7.7	14.2	7.5	10.0
13	6.2	10.3	8.3	8.5	8.6	7.1	7.3	15.3	6.6	13.9
14	6.9	10.2	7.8	9.1	8.3	6.7	7.2	12.5	6.5	8.6
15	6.7	9.1	10.4	9.9	7.4	7.6	7.3	13.1	7.2	8.3
Mean	6.47	9.44	8.45	8.77	7.55	6.76	7.45	12.37	7.34	9.49
Std Dev	0.32	0.62	0.74	0.69	0.71	0.69	0.29	1.80	0.85	1.65

LnW - 407 Resistance (kΩ)										
Insertion	**Initial**	**Thaw #1**	**Thaw #2**	**Thaw #3**	**Thaw #4**	**Thaw #5**	**Thaw #6**	**Thaw #12**	**Re-Son**	**Thaw #1**
1	7.5	9.5	9.3	9.7	8.0	6.2	7.1	15.4	5.8	9.2
2	7.1	10.5	9.1	9.3	7.4	6.7	8.2	18.3	5.9	8.0
3	7.3	9.9	8.6	10.1	8.3	7.8	7.7	16.7	5.8	9.9
4	7.4	10.6	8.2	9.4	8.8	7.9	9.0	16.0	6.2	8.9
5	7.4	10.3	8.8	10.7	7.7	6.6	8.8	17.7	7.3	9.7
6	7.6	10.5	9.5	9.5	7.8	8.0	8.1	15.3	6.5	10.1
7	7.3	9.9	8.5	9.8	8.6	6.6	7.1	16.4	8.0	9.6
8	7.6	10.0	8.7	10.7	8.4	7.5	7.9	16.2	7.4	8.7
9	7.2	10.4	8.6	9.2	7.9	7.6	7.3	15.9	8.2	10.3
10	7.3	10.0	9.0	10.8	8.9	7.7	8.2	16.1	7.3	10.2
11	7.2	10.1	8.6	8.3	7.6	6.9	8.4	16.7	7.4	9.5
12	7.9	9.5	10.8	9.0	8.1	7.7	8.8	17.2	7.5	9.7
13	7.3	9.9	8.4	10.6	8.4	7.3	7.9	16.0	7.3	10.1
14	7.1	10.0	9.4	9.7	8.3	6.9	7.3	16.4	6.5	10.2
15	7.8	11.0	10.2	9.8	9.1	7.8	8.1	15.9	6.4	10.4
Mean	7.40	10.14	9.05	9.77	8.22	7.28	7.99	16.41	6.90	9.63
Std Dev	0.24	0.41	0.71	0.71	0.50	0.58	0.61	0.81	0.79	0.68

THIS PAGE INTENTIONALLY LEFT BLANK

APPENDIX I. COMBINED CNT NANOFLUID RESISTANCE MEASUREMENTS

Mixed LnW - 402 Resistance							
L1 - 15W / 15 min, U/S with Ice bath							
Insertion	Initial	Mixed	1st Thaw	2nd Thaw	3rd Thaw	4th Thaw	5th Thaw
1	8.8	8.6	16.1	7.5	11.1	12.4	16.7
2	7.6	7.3	16.6	8.4	12.0	14.2	17.3
3	8.1	8.5	17.4	7.8	10.3	13.6	18.6
4	9.0	8.3	17.1	8.2	9.2	14.0	17.1
5	8.1	8.1	18.4	7.3	8.7	13.3	16.5
6	8.8	7.8	17.4	7.4	10.6	13.4	15.4
7	7.2	7.4	15.4	7.9	9.9	16.2	22.9
8	8.8	7.9	16.2	8.5	10.1	14.3	13.6
9	7.6	7.8	14.1	8.4	9.4	14.1	15.4
10	8.7	7.5	15.1	7.9	12.7	15.3	15.9
11	8.9	7.8	15.4	8.0	9.6	18.3	17.9
12	7.9	8.2	18.8	8.1	11.5	15.7	19.2
13	8.8	8.0	17.3	7.9	11.7	13.6	15.9
14	9.1	8.0	15.1	7.2	10.0	14.1	17.9
15	9.6	7.9	17.3	8.8	8.5	14.2	17.0
Mean	8.47	7.94	16.51	7.95	10.35	14.45	17.15
Std Dev	0.67	0.37	1.32	0.47	1.23	1.44	2.12

Notes
Max Temp during U/S - 21 °C
1st Thaw - Sediment at Bottom
2nd Thaw - Heavy Agglomerates at Bottom - Sample Unstable
3rd Thaw - Small and Large Agglomerates Suspended and Sediment at Bottom
4th Thaw - Heavy Agglomeration and Sediment at Bottom, Layered Appearance
5th Thaw - Heavy Agglomeration and Sediment at Bottom, Layered Appearance

Mixed LnW - 402 Resistance							
L2 - 15W / 15 Min, No Ice bath							
Insertion	Initial	Mixed	1st Thaw	2nd Thaw	3rd Thaw	4th Thaw	5th Thaw
1	7.8	6.6	17.6	9.0	12.1	8.4	17.2
2	8.7	7.0	18.2	8.6	14.3	8.7	16.4
3	8.9	6.3	17.4	8.7	10.9	6.3	16.8
4	8.1	6.4	18.0	9.6	10.3	7.2	15.1
5	7.4	7.4	17.0	9.5	9.9	9.2	17.9
6	8.2	7.2	16.7	8.1	10.2	11.3	16.3
7	9.0	5.2	19.1	9.8	10.0	11.8	18.1
8	8.4	6.0	14.7	9.3	11.2	13.2	17.0
9	8.3	5.5	15.9	9.0	10.7	14.6	15.6
10	9.2	6.2	17.9	10.0	15.8	16.8	15.0
11	8.1	5.4	16.7	9.4	12.0	16.2	16.8
12	9.1	5.0	15.6	8.3	13.3	13.6	17.3
13	9.0	4.7	18.2	9.0	10.3	13.8	19.4
14	8.4	6.1	16.2	8.9	14.6	14.0	15.8
15	7.8	5.2	15.5	8.5	13.3	15.0	17.4
Mean	8.43	6.01	16.98	9.05	11.93	12.01	16.81
Std Dev	0.54	0.83	1.23	0.55	1.90	3.33	1.18

Notes
Max Temp during U/S - 72 °C
1st Thaw - Sediment at Bottom
2nd Thaw - Small Agglomerate Suspensions and Sediment at Bottom
3rd Thaw - Small Agglomerates and Sediment at Bottom
4th Thaw - Small Agglomerates and Suspensions with Sediment at Bottom
5th Thaw - Small Agglomerates and Suspensions with Sediment at Bottom

*All Resistances in kilo-ohm

Mixed LnW - 402 Resistance							
L3 - 39 W / 15 Min, U/S with Ice Bath							
Insertion	Initial	Mixed	1st Thaw	2nd Thaw	3rd Thaw	4th Thaw	5th Thaw
1	8.4	7.4	16.6	9.1	15.0	15.8	21.3
2	7.8	7.3	17.1	9.2	13.0	16.2	22.6
3	9.0	7.2	18.9	9.4	13.3	16.3	18.0
4	9.1	6.0	15.1	9.2	14.2	19.0	17.5
5	8.1	6.9	16.2	10.2	12.3	16.8	16.7
6	8.2	7.2	18.0	9.8	15.6	17.1	18.4
7	8.9	7.1	15.1	9.5	10.4	17.0	16.6
8	8.7	7.7	17.8	9.2	11.6	15.8	17.8
9	9.6	8.1	17.5	8.4	13.6	16.9	18.3
10	10.1	6.7	16.4	8.7	11.7	16.2	23.2
11	8.1	7.0	16.9	8.1	14.0	15.9	15.2
12	8.7	8.1	15.5	9.5	12.5	18.4	18.9
13	8.2	7.4	16.0	8.8	14.1	17.2	23.4
14	8.6	7.7	18.5	9.0	14.6	19.2	17.2
15	8.4	8.0	16.8	8.3	15.3	18.0	15.9
Mean	8.66	7.32	16.83	9.09	13.41	17.05	18.73
Std Dev	0.61	0.56	1.16	0.57	1.50	1.12	2.65

Notes
Max Temp during U/S - 34 °C
1st Thaw - Minor Sediment at Bottom
2nd Thaw - Heavy Agglomeration at Bottom - Sample Unstable
3rd Thaw - Small and Large Agglomerates Suspended and Sediment at Bottom
4th Thaw - Large Agglomerates and Suspensions with Sediment at Bottom
5th Thaw - Large Agglomerates and Suspensions with Sediment at Bottom

Mixed LnW - 402 Resistance							
L4 - 39W / 15 Min, No Ice bath							
Insertion	Initial	Mixed	1st Thaw	2nd Thaw	3rd Thaw	4th Thaw	5th Thaw
1	8.5	5.0	17.4	8.3	13.8	14.3	17.9
2	9.0	4.9	18.3	9.5	11.4	15.6	20.1
3	7.2	5.6	17.1	8.6	12.7	17.8	17.1
4	7.3	4.9	17.3	8.8	8.7	17.2	15.2
5	7.4	5.8	20.1	8.9	11.4	17.5	18.5
6	8.6	5.7	22.3	7.9	9.9	18.1	19.5
7	9.2	5.5	15.4	8.5	8.0	16.2	22.9
8	8.5	5.2	18.3	8.3	8.8	19.1	20.4
9	7.4	4.8	16.2	9.3	12.7	16.8	19.2
10	8.3	5.5	19.6	9.5	12.4	18.0	19.0
11	8.5	5.9	18.2	8.5	12.9	19.1	21.8
12	7.4	6.4	19.8	8.4	12.0	17.2	18.2
13	8.3	6.2	15.7	9.8	11.9	19.2	16.9
14	8.5	5.6	17.7	9.3	14.3	18.4	19.1
15	7.6	6.0	18.1	8.6	13.0	19.2	19.0
Mean	8.11	5.53	18.10	8.81	11.59	17.58	18.99
Std Dev	0.66	0.49	1.81	0.55	1.91	1.43	1.91

Notes
Max Temp during U/S - 78 °C
1st Thaw - Heavy Sediment and agglomeration at Bottom - Sample Unstable
2nd Thaw - Heavy Sediment and agglomeration at Bottom
3rd Thaw - Heavy Sediment and agglomeration at Bottom
4th Thaw - Heavy Sediment and agglomeration at Bottom
5th Thaw - Heavy Sediment and agglomeration at Bottom

*All Resistances in kilo-ohm

Mixed LnW - 405 Resistance							
L5 - 15W / 15 min, U/S with Ice bath							
Insertion	**Initial**	**Mixed**	**1st Thaw**	**2nd Thaw**	**3rd Thaw**	**4th Thaw**	**5th Thaw**
1	8.4	7.5	11.8	15.2	12.5		
2	7.4	7.3	9.9	16.6	11.7		
3	7.8	7.8	10.1	11.5	11.1		
4	7.6	7.1	9.2	16.8	9.3		
5	7.9	6.8	8.7	9.8	13.9		
6	7.3	7.1	9.8	12.5	9.0		
7	8.0	7.0	11.6	10.8	13.0		
8	7.9	8.0	8.6	10.6	10.5		
9	8.8	7.1	9.1	9.1	10.1		
10	6.8	7.6	7.7	10.6	11.5		
11	7.8	7.1	10.5	9.6	14.9		
12	7.5	7.7	8.8	9.7	10.3		
13	7.7	6.8	8.9	13.6	11.3		
14	7.4	6.6	9.2	11.7	10.7		
15	9.6	8.5	9.3	10.8	9.3		
Mean	7.86	7.33	9.55	11.93	11.27	#DIV/0!	#DIV/0!
Std Dev	0.67	0.51	1.11	2.52	1.71	#DIV/0!	#DIV/0!

Notes

Max Temp during U/S - 20°C

1st Thaw - Minor Sediment at Bottom

2nd Thaw - Layered Appearance, Sample Unstable, Heavy Agglomeration and Sediment at Bottom

3rd Thaw - Layered Appearance, Sample Unstable, Heavy Agglomeration and Sediment at Bottom

Mixed LnW - 405 Resistance							
L6 - 15W / 15 Min, No Ice bath							
Insertion	Initial	Mixed	1st Thaw	2nd Thaw	3rd Thaw	4th Thaw	5th Thaw
1	7.7	3.9	10.7	14.1	12.6		
2	8.5	4.0	8.8	13.4	9.7		
3	8.6	4.6	9.0	11.4	10.7		
4	8.1	4.0	8.8	14.0	9.9		
5	7.9	4.8	9.7	10.8	9.3		
6	8.3	3.8	9.0	9.2	10.0		
7	8.0	4.2	9.1	9.6	8.1		
8	8.3	4.0	9.7	8.8	8.2		
9	6.8	3.8	8.7	13.9	12.1		
10	9.7	3.6	7.6	10.6	8.7		
11	7.6	3.9	9.5	10.3	7.7		
12	10.0	3.7	11.3	9.3	8.0		
13	8.4	3.9	8.2	9.5	9.3		
14	8.0	4.0	8.4	8.7	8.9		
15	8.2	4.3	7.6	13.6	11.7		
Mean	8.27	4.03	9.07	11.15	9.66	#DIV/0!	#DIV/0!
Std Dev	0.78	0.32	1.02	2.08	1.53	#DIV/0!	#DIV/0!

Notes
Max Temp during U/S - 69 °C
1st Thaw - Minor Sediment at Bottom
2nd Thaw - Layered Appearance, Sample Unstable, Heavy Agglomeration and Sediment at Bottom
3rd Thaw - Layered Appearance, Sample Unstable, Heavy Agglomeration and Sediment at Bottom

*All Resistances in kilo-ohm

Mixed LnW - 405 Resistance							
L7 - 39 W / 15 Min, U/S with Ice Bath							
Insertion	Initial	Mixed	1st Thaw	2nd Thaw	3rd Thaw	4th Thaw	5th Thaw
1	6.8	6.1	8.7	15.4	7.5		
2	7.3	5.7	6.9	9.4	7.8		
3	7.7	5.5	7.8	11.6	8.8		
4	6.6	5.8	7.1	9.0	8.3		
5	7.5	6.0	7.6	7.9	10.5		
6	7.3	5.7	8.5	9.1	9.0		
7	7.5	6.0	9.2	9.3	8.3		
8	7.0	5.4	8.1	9.1	7.3		
9	7.2	5.7	8.6	9.5	10.5		
10	8.6	6.2	9.0	9.6	7.6		
11	10.0	7.0	6.5	15.4	8.9		
12	8.4	7.5	8.3	8.8	10.7		
13	7.5	7.0	8.5	10.0	9.6		
14	8.4	6.2	8.3	9.9	9.1		
15	7.2	5.7	7.5	8.4	10.4		
Mean	7.67	6.10	8.04	10.16	8.95	#DIV/0!	#DIV/0!
Std Dev	0.87	0.61	0.79	2.28	1.17	#DIV/0!	#DIV/0!

Notes
Max Temp during U/S - 43 °C
1st Thaw - Minor Sediment at Bottom
2nd Thaw - Layered Appearance, Sample Unstable, Heavy Agglomeration and Sediment at Bottom
3rd Thaw - Layered Appearance, Sample Unstable, Heavy Agglomeration and Sediment at Bottom

Mixed LnW - 405 Resistance							
L8 - 39W / 15 Min, No Ice bath							
Insertion	**Initial**	**Mixed**	**1st Thaw**	**2nd Thaw**	**3rd Thaw**	**4th Thaw**	**5th Thaw**
1	6.7	6.2	8.9	7.8	11.0		
2	7.3	5.4	7.9	8.2	10.5		
3	7.0	5.8	7.6	8.4	9.6		
4	7.8	7.5	8.0	7.4	9.0		
5	6.8	6.4	6.9	8.5	10.7		
6	7.1	5.4	6.6	9.1	8.2		
7	8.2	5.0	7.8	10.0	7.6		
8	7.5	5.6	7.9	9.4	9.5		
9	8.7	5.3	9.7	8.5	8.1		
10	7.1	5.7	8.5	8.6	10.0		
11	6.8	5.0	11.4	9.1	8.3		
12	6.9	6.4	8.5	8.1	9.1		
13	7.4	5.6	9.7	9.9	7.9		
14	7.2	5.9	8.1	10.6	9.4		
15	7.9	5.2	9.0	9.1	11.3		
Mean	7.36	5.76	8.43	8.85	9.35	#DIV/0!	#DIV/0!
Std Dev	0.57	0.66	1.20	0.87	1.18	#DIV/0!	#DIV/0!

Notes

Max Temp during U/S - 84 °C

1st Thaw - Heavy Sediment and agglomeration at Bottom

2nd Thaw - Layered Appearance, Sample Unstable, Heavy Agglomeration and Sediment at Bottom

3rd Thaw - Layered Appearance, Sample Unstable, Heavy Agglomeration and Sediment at Bottom

THIS PAGE INTENTIONALLY LEFT BLANK

LIST OF REFERENCES

[1] J. C. Maxwell, *Electricity and Magnetism, Part 2.*, 3rd ed. United Kingdom: Clarendon Press, 1904.

[2] S. U. S. Choi, "Nanofluid Technology: Current Status and Future Research," Argonne National Laboratory, Argonne, Illinois, Tech. Rep. 97466, 1999.

[3] J. A. Eastman, S. R. Phillpot, S. U. S. Choi, and P. Keblinski, "Thermal Transport in Nanofluids," *Annual Review of Materials Science,* pp. 219, 2004.

[4] J. Li and C. Kleinstreuer, "Thermal Performance of Nanofluid Flow in Microchannels," *International Journal of Heat and Fluids Flow,* pp. 1221, 2008.

[5] X. Wang and A. S. Mujumdar, "A Review on Nanofluids—Part II: Experiments and Applications," *Brazilian Journal of Chemical Engineering,* vol. 25, pp. 631, 2008.

[6] S. U. S. Choi and J. A. Eastman, "Enhancing Thermal Conductivity of Fluids with Nanoparticles," Argonne National Laboratory, Illinois, Tech. Rep. ANL/ET/CP--88239; CONF-951135--29, 1995.

[7] E. T. Swartz and R. O. Pohl, "Thermal Boundary Resistance," *Review of Modern Physics,* vol. 61, 1989.

[8] S. Iijima, "Helical Microtubules of Graphitic Carbon," in *Nature.* Anonymous 1991, pp. 56–354.

[9] Penn Engineering, "Carbon Nanotube," 2009.

[10] Web site Graphic: http://www.antnanousa.cn "SWCNT & MWCNT," 2009.

[11] M. S. Dresselhaus and G. Dresselhaus, *Carbon Nanotubes: Properties, Synthesis, Structure and Applications.* New York: Springer, 2001.

[12] H. Xie, H. Lee, W. Youn, and M. Choi, "Nanofluids Containing Mulitwalled Carbon Nanotubes and Their Enhanced Thermal Conductivities," *Journal of Applied Physics,* vol. 94, pp. 4967, 2003.

[13] D. Wen and Y. Ding, "Effective Thermal Conductivity of Aqueous Suspensions of Carbon Nanotubes (Carbon Nanotube Nanofluids)," *Journal of Thermophysics and Heat Transfer,* vol. 18, 2004.

[14] M. J. Assael, C. F. Chen, I. Metaxa, and W. A. Wakeham, "Thermal Conductivity of Suspensions of Carbon Nanotubes in Water," *International Journal of Thermophysics,* vol. 25, pp. 971, 2004.

[15] F. D. S. Marquis and L. P. F. Chilbante, "Improving the Heat Transfer of Nanofluids and Nanolubricants with Carbon Nanotubes," *JOM,* pp. 32, 2005.

[16] M. Bahrami, M. M. Yovanovich, and J. R. Culham, "Assessment of Relevant Physical Phenomena Controlling Thermal Performance of Nanofluids," *Journal of Thermophysics and Heat Transfer,* vol. 21, 2007.

[17] S. Joslin, "Nanofluids," 2009.

[18] A. Jorio, G. Dresselhaus, and M. S. Dresselhaus, *Carbon Nanotubes: Advanced Topics in the Synthesis, Structure, Properties and Application*, 1st ed.Springer, 2008.

[19] J. A. Kuhlmann, "Development of Thermal Management Systems for High Energy Applications," Master's thesis, Naval Postgraduate School, Monterey, CA 2008.

[20] The International Association for the Properties of Water and Steam, "Guidelines on the Use of Fundamental Physical Constants and Basic Constants of Water," 2001.

[21] Web site: Nano-Lab Incorporated, Internet Home Page, http://www.nano-lab.com/nanotubes-research-grade.html, 2009.

[22] Web site: Sigma-Aldrich, Internet Home Page, http://www.sigmaaldrich.com/sigma-aldrich/home.html, 2009.

[23] American Society of Testing and Materials International, "Standard Test Methods for Electrical Conductivity and Resistivity of Water," ASTM International, Tech. Rep. D1125-95, 2009.

[24] T. S. Light, S. Licht, A. C. Bevilacqua, and K. R. Morashc, "The Fundamental Conductivity and Resistivity of Water," *Electrochemical and Solid-State Letters,* vol. 8, pp. E16, 2005.

BIBLIOGRAPHY

Nano-lab Incorporated Home Page. 2009 [cited 11/14 2009]. Available from http://www.nano-lab.com/nanotubes-research-grade.html.

Sigma-aldrich Home Page. 2009 [cited 08/15 2009]. Available from http://www.sigmaaldrich.com/sigma-aldrich/home.html.

SWCNT & MWCNT. [cited 11/12 2009]. Available from http://images.google.com/imgres?imgurl=http://www.antnanousa.cn/dev/samples/images/thumb/mwnt.gif&imgrefurl=http://www.antnanousa.cn/dev/samples/nanotubes.asp&usg=___wC77ILUkrHc5yMksEMHvvr419s=&h=147&w=160&sz=13&hl=en&start=10&um=1&itbs=1&tbnid=8mkhHKhqIrZYqM:&tbnh=90&tbnw=98&prev=/images%3Fq%3DMWNT%2Band%2BSWNT%2Bpicture%26hl%3Den%26sa%3DN%26um%3D1.

American Society of Testing and Materials International. 2009. *Standard Test Methods for Electrical Conductivity and Resistivity of Water.* ASTM International, D1125-95.

Assael, M. J., C. F. Chen, I. Metaxa, and W. A. Wakeham. 2004. Thermal conductivity of Suspensions of Carbon Nanotubes in Water. *International Journal of Thermophysics* 25, (4): 971.

Bahrami, Majid, M. M. Yovanovich, and J. R. Culham. 2007. Assessment of Relevant Physical Phenomena Controlling Thermal Performance of Nanofluids. *Journal of Thermophysics and Heat Transfer* 21, (4).

Bigg, Donald M. 1979. Mechanical, Thermal and Electrical Properties of Metal Fiber-filled Polymer Composites. *Polymer Engineering and Science* 19, (16).

Choi, S. U. S. 1999. *Nanofluid technology: Current Status and Future Research.* Argonne, Illinois: Argonne National Laboratory, 97466.

Choi, S. U. S. and J. A. Eastman. 1995. *Enhancing Thermal Conductivity of Fluids with Nanoparticles.* Illinois: Argonne National Laboratory, ANL/ET/CP--88239; CONF-951135--29.

Choi, S. U. S., Z. G. Zhang, W. Yu, F. E. Lockwood, and E. A. Grulke. 2001. Anomalous Thermal Conductivity Enhancement in Nanotube Suspensions. *Applied Physics Letters* 79, (14): 2252.

Dresselhaus, M. S. and G. Dresselhaus. 2001. *Carbon Nanotubes: Properties, Synthesis, Structure and Applications,* ed. Ph Avouris. New York: Springer.

Eastman, J. A., S. R. Phillpot, S. U. S. Choi, and P. Keblinski. 2004. Thermal Transport in Nanofluids. *Annual Review of Materials Science*(August): 219.

Grace, Tom. 2003. *An Introduction to Carbon Nanotubes*.

Hong, Haiping, Jesse Wensel, Feng Liang, W. E. Billups, and Walter Roy. 2006. Heat Transfer Nanofluids Based on Carbon Nanotubes. *American Institute of Aeronautics and Astronautics*(June).

Hong, Haiping, Jesse Wensel, Shelley Peterson, and Walter Roy. 2007. Efficiently Lowering the Freezing Point in Heat Transfer Coolants Using Carbon Nanotubes. *Journal of Thermophysics and Heat Transfer* 21, (2).

Iijima, S. 1991. Helical Microtubules of Graphitic Carbon. In *Nature*, 56-354.

Jorio, A., G. Dresselhaus, and M. S. Dresselhaus. 2008. *Carbon Nanotubes: Advanced Topics in the Synthesis, Structure, Properties and Application*, eds. G. Dresselhaus, M. S. Dresselhaus. 1st ed.Springer.

Joslin, S. 2009. Nanofluids. Luna Innovations, Danville, Virginia.

Kim, Bong Hun, and G. P. Peterson. 2007. Effect of Morphology of Carbon Nanotubes on Thermal Conductivity Enhancement of Nanofluids. *Journal of Thermophysics and Heat Transfer* 21, (3).

Kuhlmann, James A. 2008. Development of Thermal Management Systems for High Energy Applications. Master's thesis, Naval Postgraduate School, Monterey, CA.

Lee, Shinpyo and S. U. S. Choi. 1996. Application of Metallic Nanoparticle Suspensions in Advanced Cooling Systems. Paper presented at International Mechanical Engineering Conference, Atlanta, GA.

Li, Jie and Clement Kleinstreuer. 2008. Thermal Performance of Nanofluid Flow in Microchannels. *International Journal of Heat and Fluids Flow* (January): 1221.

Light, T. S., S. Licht, A. C. Bevilacqua, and K. R. Morashc. 2005. The Fundamental Conductivity and Resistivity of Water. *Electrochemical and Solid-State Letters* 8, (1): E16.

Liu, Zhen-Hua and Lin Lu. 2009. Thermal Performance of an Axially Microgrooved Heat Pipe Using Carbon Nanotube Suspensions. *Journal of Thermophysics and Heat Transfer* 23, (1).

Marquis, F. D. S. and L. P. F. Chilbante. 2005. Improving the Heat Transfer of Nanofluids and Nanolubricants with Carbon Nanotubes. *JOM*(December): 32.

Maxwell, J. C. 1904. *Electricity and Magnetism, part 2*. 3rd ed. United Kingdom: Clarendon Press.

Penn Engineering. Carbon Nanotube. [cited 11/06 2009]. Available from http://www.seas.upenn.edu/mse/images/nanotube1.jpg.

Rahman, Muhammad M. and Shantanu S. Shevade. 2003. Microchannel Thermal Management During Volumetric Heating or Cooling. *American Institute of Aeronautics and Astronautics* (August).

Swartz, E. T. and R. O. Pohl. 1989. Thermal Boundary Resistance. *Review of Modern Physics* 61, (3).

The International Association for the Properties of Water and Steam. 2001. *Guideline on the Use of Fundamental Physical Constants and Basic Constants of Water*. International Association for the Properties of Water and Steam.

Wang, Xiang-Qi and Arun S. Mujumdar. 2008. A Review on Nanofluids - Part II: Experiments and Applications. *Brazilian Journal of Chemical Engineering* 25, (4): 631.

Wen, Dongsheng and Yulong Ding. 2004. Effective Thermal Conductivity of Aqueous Suspensions of Carbon Nanotubes (Carbon Nanotube Nanofluids). *Journal of Thermophysics and Heat Transfer* 18, (4).

Xie, H., H. Lee, W. Youn, and M. Choi. 2003. Nanofluids Containing Mulitwalled Carbon Nanotubes and Their Enhanced Thermal Conductivities. *Journal of Applied Physics* 94, (8): 4967.

Young, Stuart H. 1996. An Optimization Technique Using the Finite Element Method and Orthogonal Arrays. M.S. in Mechanical Engineering., Naval Postgraduate School, Monterey, CA, http://edocs.nps.edu/npspubs/scholarly/theses/1996/Sep/96Sep_Young.pdf

THIS PAGE INTENTIONALLY LEFT BLANK

INITIAL DISTRIBUTION LIST

1. Defense Technical Information Center
   Ft. Belvoir, Virginia

2. Dudley Knox Library
   Naval Postgraduate School
   Monterey, California

3. Research Office, Code 41
   Naval Postgraduate School
   Monterey, California

4. David Rummler
   Northrop Grumman Systems Corporation, Electronic Systems Sector (NGES)
   Marine Systems Business Unit
   401 East Hendy Avenue
   Sunnyvale, California 94088

5. Young W. Kwon, Professor
   Naval Postgraduate School
   Dept. of Mechanical & Astronautical Engineering
   Monterey, California

6. Randall Pollak, Major USAF
   Asst Professor, Space Systems Academic Group
   Naval Postgraduate School
   Dept. of Mechanical & Astronautical Engineering
   Monterey, California

6. Brian Ryglowski, LT USN
   Naval Postgraduate School
   Monterey, California